

38772-101



REPORT DOCUMENTATION PAGE		1. REPORT NO. NCEER-92-0025	2.	3. PB93-227791
4. Title and Subtitle Experimental Results of Repaired and Retrofitted Beam-Column Joint Tests in Lightly Reinforced Concrete Frame Buildings			5. Report Date October 29, 1992	
7. Author(s) A. Beres, S. El-Borgi, R.N. White and P. Gergely			6. Performing Organization Rept. No.	
9. Performing Organization Name and Address Department of Structural Engineering School of Civil and Environmental Engineering Cornell University Ithaca, New York 14853-3501			10. Project/Task/Work Unit No.	
			21. Contract/Grant/Order No. BCS 90-25010 NEC-91029	
13. Sponsoring Organization Name and Address National Center for Earthquake Engineering Research State University of New York at Buffalo Red Jacket Quadrangle Buffalo, New York 14261			12. Type of Report & Period Covered Technical Report	
			14.	
15. Supplementary Notes This research was conducted at Cornell University and was partially supported by the National Science Foundation under Grant No. BCS 90-25010 and the New York State Science and Technology Foundation under Grant No. NEC-91029.				
16. Abstract (Limit: 200 words) This report summarizes current experimental work at Cornell University concerning lightly reinforced concrete structures. The report includes: 1) a brief summary of the full-scale experiments conducted on the behavior of lightly reinforced concrete building frame components subjected to reversing cyclic loads (simulated seismic effects); 2) description of experimental findings on a repaired interior joint; and 3) results of tests on two retrofitted frame joint regions. A total of 34 interior and exterior beam-column joints were tested to identify the different damage mechanisms and study the effect of critical details. The most important findings on the behavior of various types of specimens are summarized in Section 3. One of the already tested interior specimens was repaired and retested. The repair method chosen in this case was vacuum resin injection as described in Section 4. Finally, two virgin specimens (one interior and one exterior) were retrofitted with externally attached steel plates as discussed in Section 5.				
17. Document Analysis a. Descriptors				
b. Identifiers/Open-Ended Terms Lightly reinforced concrete frames. Gravity load design. Full scale tests. Beam column joints. Earthquake engineering. Damage mechanisms. Reversed cyclic loads.				
c. OSBAT Field/Group				
18. Availability Statement Release Unlimited		19. Security Class (This Report) Unclassified		20. No. of Pages 84
		21. Security Class (This Page) Unclassified		22. Price



**NATIONAL CENTER FOR EARTHQUAKE
ENGINEERING RESEARCH**

State University of New York at Buffalo



PB93 - 227791

**Experimental Results of Repaired and
Retrofitted Beam-Column Joint Tests
in Lightly Reinforced Concrete Frame Buildings**

by

A. Beres, S. El-Borgi, R.N. White and P. Gergely

**Department of Structural Engineering
School of Civil and Environmental Engineering
Cornell University
Ithaca, New York 14853-3501**

Technical Report NCEER-92-0025

October 29, 1992

This research was conducted at Cornell University and was partially supported by the National Science Foundation under Grant No. BCS 90-25010 and the New York State Science and Technology Foundation under Grant No. NEC-91029.

NOTICE

This report was prepared by Cornell University as a result of research sponsored by the National Center for Earthquake Engineering Research (NCEER) through grants from the National Science Foundation, the New York State Science and Technology Foundation, and other sponsors. Neither NCEER, associates of NCEER, its sponsors, Cornell University, nor any person acting on their behalf:

- a. makes any warranty, express or implied, with respect to the use of any information, apparatus, method, or process disclosed in this report or that such use may not infringe upon privately owned rights; or
- b. assumes any liabilities of whatsoever kind with respect to the use of, or the damage resulting from the use of, any information, apparatus, method or process disclosed in this report.

Any opinions, findings, and conclusions or recommendations expressed in this publication are those of the author(s) and do not necessarily reflect the views of the National Science Foundation, the New York State Science and Technology Foundation, or other sponsors.



PB93-227791

**Experimental Results of Repaired and
Retrofitted Beam-Column Joint Tests
in Lightly Reinforced Concrete Frame Buildings**

by

A. Beres¹ S. El-Borgi¹, R.N. White² and P. Gergely³

October 29, 1992

Technical Report NCEER-92-0025

NCEER Project Number 91-3111A

NSF Master Contract Number BCS 90-25010

and

NYSSTF Grant Number NEC-91029

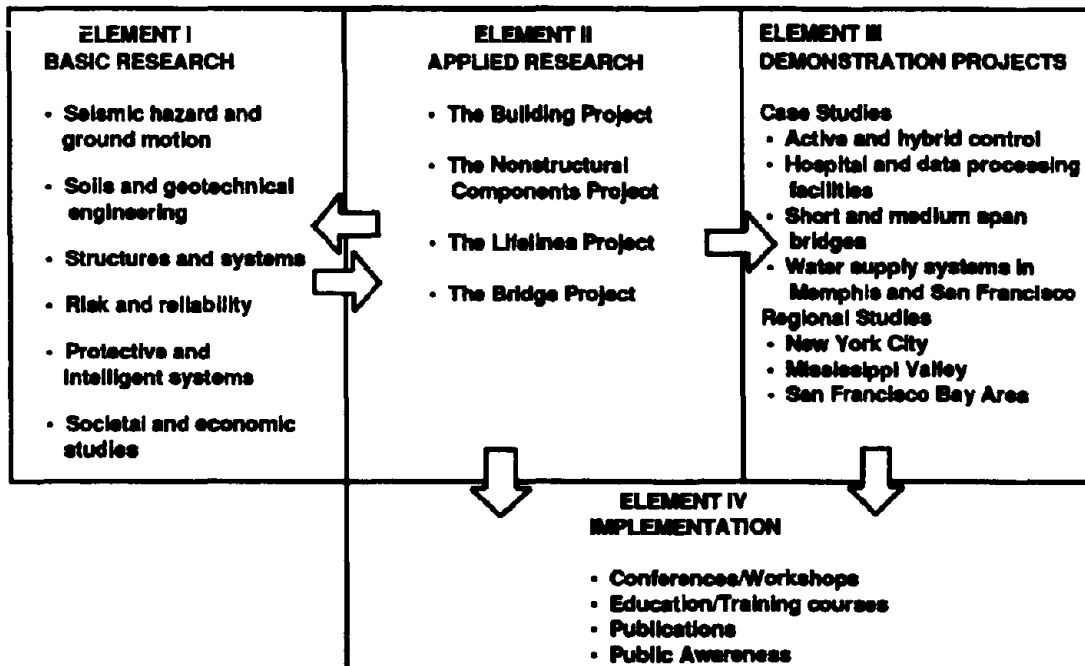
- 1 Graduate Research Assistant, School of Civil and Environmental Engineering, Cornell University
- 2 James A. Friend Family Professor of Engineering, School of Civil and Environmental Engineering, Cornell University
- 3 Professor of Structural Engineering, School of Civil and Environmental Engineering, Cornell University

NATIONAL CENTER FOR EARTHQUAKE ENGINEERING RESEARCH
State University of New York at Buffalo
Red Jacket Quadrangle, Buffalo, NY 14261

PREFACE

The National Center for Earthquake Engineering Research (NCEER) was established to expand and disseminate knowledge about earthquakes, improve earthquake-resistant design, and implement seismic hazard mitigation procedures to minimize loss of lives and property. The emphasis is on structures in the eastern and central United States and lifelines throughout the country that are found in zones of low, moderate, and high seismicity.

NCEER's research and implementation plan in years six through ten (1991-1996) comprises four interlocked elements, as shown in the figure below. Element I, Basic Research, is carried out to support projects in the Applied Research area. Element II, Applied Research, is the major focus of work for years six through ten. Element III, Demonstration Projects, have been planned to support Applied Research projects, and will be either case studies or regional studies. Element IV, Implementation, will result from activity in the four Applied Research projects, and from Demonstration Projects.



Research in the **Building Project** focuses on the evaluation and retrofit of buildings in regions of moderate seismicity. Emphasis is on lightly reinforced concrete buildings, steel semi-rigid frames, and masonry walls or infills. The research involves small- and medium-scale shake table tests and full-scale component tests at several institutions. In a parallel effort, analytical models and computer programs are being developed to aid in the prediction of the response of these buildings to various types of ground motion.

ABSTRACT

This report summarizes the current experimental work at Cornell University concerning lightly reinforced concrete structures. Lightly reinforced concrete framing, designed primarily for the effects of gravity loads with little or no attention given to lateral load effects, is characterized by the following details: no more than about 2% longitudinal column reinforcement with lap splices located immediately above floor levels in the zone of maximum seismic moment, widely spaced column ties, little or no transverse reinforcement within the joint region, columns having bending moment capacity close to those of the beams, and discontinuous positive moment beam reinforcement with six inches embedment length into the column.

This report includes: (a) a brief summary of the full-scale experiments conducted on the behavior of lightly reinforced concrete building frame components subjected to reversing cyclic loads (simulated seismic effects), (b) description of experimental findings on a repaired interior joint, and (c) results of tests on two retrofitted frame joint regions.

A total of 34 interior and exterior beam-column joints were tested to identify the different damage mechanisms and study the effect of critical details. The most important findings on the behavior of various types of specimens are summarized in Section 3. One of the already tested interior specimens was repaired and retested. The repair method chosen in this case was vacuum resin injection as described in Section 4. Finally, two virgin specimens (one interior and one exterior) were retrofitted with externally attached steel plates as discussed in Section 5.

ACKNOWLEDGMENTS

This research was sponsored by the National Institute of Standards and Technology and the National Center of Earthquake Engineering Research with funding from the National Science Foundation and the New York State Science and Technology Foundation.

Advice in earlier phases of the NCEER program was received from numerous practicing engineers. Input on retrofit schemes from Jacob Grossman of Robert Rossenwasser Associates of New York City was greatly appreciated. The authors wish to express their appreciation to Balvac Incorporated of Buffalo, NY, for contributing time, material, and equipment in applying their resin vacuum injection technology, and in particular for the valuable consultations with James Gallo, James Villar, Keith Davis, and Icky Haq. Williams Form Engineering Corporation of Grand Rapids, MI, donated the adhesive anchor system and advised on installation procedures for the retrofit scheme of the interior specimen. Comments on the manuscript received from Dr. Long Phan of NIST and Professor Andrei Reinhorn of SUNY Buffalo were also very helpful.

Special thanks are due to Tim Bond and David Farmer of the George Winter Laboratory Technical Services, and to Paul Jones and John Yost of Cornell Civil Engineering Machine Shop. Thanks are also extended to the many undergraduate laboratory assistants who helped at various phases of the experimental work.

A note of thanks is given to the faculty members and the graduate students of the State University of New York at Buffalo who are collaborators in the NCEER Lightly Reinforced Concrete Structures Research Group. Their contributions in computer simulation and experimental evaluation of reinforced concrete frames provided substantial support for the efforts at Cornell.

Opinions expressed herein are those of the authors only and not of the sponsors.

TABLE OF CONTENTS

SECTION	TITLE	PAGE
1.	Introduction and Scope of Report	1-1
2.	Experimental Program	2-1
2.1	Identification of Critical Details.....	2-1
2.2	Specimen Geometry and Fabrication Details.....	2-2
2.3	Loading Arrangement	2-3
2.4	Measurement and Control Systems	2-3
3.	Experimentally Observed Behavior of Lightly Reinforced Beam–Column Joints Without Retrofit	3-1
3.1	Interior Joint Regions with Continuous Bottom Beam Reinforcement	3-1
3.2	Interior Joint Regions with Discontinuous Bottom Beam Reinforcement	3-3
3.3	Exterior Joint Regions with Discontinuous Bottom Beam Reinforcement	3-5
4.	Seismic Repair Scheme.....	4-1
4.1	Introduction.....	4-1
4.2	Evaluation of Test Results and Comparisons with Non–repaired Specimens	4-1
4.2.1	Repair Scheme.....	4-3
4.2.2	General Behavior of Repaired Specimen and Damage Progress	4-5
4.2.3	Specimen Strength and Interstory Drift	4-8
4.2.4	Specimen Stiffness.....	4-9
4.2.5	Energy Dissipation.....	4-10
4.3	Summary	4-11
5.	Seismic Retrofit Schemes.....	5-1
5.1	Introduction.....	5-1
5.2	Interior Joint	5-2
5.2.1	Retrofit Scheme.....	5-2
5.2.2	Evaluation of Test Results and Comparisons with Non–retrofitted Specimens	5-4
5.2.2.1	General Behavior and Damage Progress	5-5
5.2.2.2	Specimen Strength and Interstory Drift	5-7
5.2.2.3	Stresses in the Connecting Tie–bars	5-7
5.2.2.4	Specimen Stiffness	5-9

5.2.2.5	Energy Dissipation.....	5-11
5.2.3	Summary.....	5-12
5.3	Exterior Joint.....	5-12
5.3.1	Retrofit Scheme.....	5-12
5.3.2	Evaluation of Test Results and Comparisons with Non-retrofitted Specimens.....	5-13
5.3.2.1	General Behavior and Damage Progress.....	5-14
5.3.2.2	Specimen Strength and Interstory Drift.....	5-15
5.3.2.3	Specimen Stiffness.....	5-18
5.3.2.4	Energy Dissipation.....	5-19
5.3.3	Summary.....	5-20
6.	Summary, Conclusions, and Suggestions for Future Research.....	6-1
6.1	Summary and Conclusions.....	6-1
6.1.1	Repaired Specimen.....	6-1
6.1.2	Retrofitted Specimens.....	6-2
6.2	Recommendations for Future Research.....	6-4
7.	References.....	7-1
	Appendix.....	A-1
A.	Technical Comments about Adhesive Anchor Installation.....	A-1

LIST OF ILLUSTRATIONS

FIGURE #	TITLE	PAGE
2-1	Elevation View of an Interior and an Exterior Beam-Column Connection Region.....	2-2
2-2	Photo of the Testing Frame.....	2-4
2-3	Two Elevation Views of the Testing Frame.....	2-5
2-4	Idealization of the Force and Reaction System.....	2-5
2-5	Typical Load History.....	2-6
2-6	Arrangement of Instrumentation (DCDTs) for a Typical Interior Specimen (I-11) with Gravity Load On.....	2-7
3-1	Typical Interior Joint with Continuous Reinforcement.....	3-2
3-2	Typical Interior Joint with Discontinuous Reinforcement.....	3-4
3-3	Typical Exterior Joint with Discontinuous Reinforcement.....	3-7
4-1	Specimen Reinforcement and Dimensions.....	4-2
4-2	Implementation of the Repair.....	4-4
4-3	Cracking Patterns.....	4-6
4-4	Photo Taken After the Test.....	4-7
4-5	Column Shear Force Versus Interstory Drift Before and After Repair.....	4-8
4-6	Bending Moment Versus Rotation in Beams Before and After Repair.....	4-9
4-7	Stiffness vs. Maximum Interstory Drift Before and After Repair.....	4-10
4-8	Cumulative Energy Dissipation vs. Interstory Drift Before and After Repair.....	4-10
5-1	Retrofit Configuration (interior).....	5-3
5-2	Specimen Reinforcement and Dimensions (interior).....	5-5
5-3	Cracking Patterns (interior).....	5-6
5-4	Photo Taken After the Test (interior).....	5-8
5-5	Column Shear Force Versus Interstory Drift (interior).....	5-9
5-6	Column Shear Force Versus Interstory Drift Envelopes (interior).....	5-9
5-7	Longitudinal Stress in the Tie-bars (interior).....	5-10
5-8	Stiffness vs. Maximum Interstory Drift (interior).....	5-10
5-9	Cumulative Energy Dissipation vs. Interstory Drift (interior).....	5-11
5-10	Retrofit Configuration (exterior).....	5-13
5-11	Specimen Reinforcement and Dimensions (exterior).....	5-14
5-12	Cracking Patterns (exterior).....	5-15
5-13	Photo Taken After the Test (exterior).....	5-16
5-14	Column Shear-Interstory Drift (exterior).....	5-17

5-15	Column Shear Force Versus Interstory Drift Envelopes (exterior).....	5-17
5-16	Stiffness vs. Maximum Interstory Drift (exterior).....	5-18
5-17	Cumulative Energy Dissipation vs. Interstory Drift (exterior).....	5-19

SECTION 1

INTRODUCTION AND SCOPE OF REPORT

There are many thousands of multistory reinforced concrete frame structures in the United States that were designed without regard to any significant lateral forces. The lateral load resistance of these structures is considered suspect for even moderate earthquakes because the non-ductile reinforcing details used are in sharp contrast to the design approaches currently applied in modern seismic design.

To develop reliable seismic evaluation techniques for this class of frames, a comprehensive experimental and analytical research program has been underway at Cornell University under the auspices of the National Center for Earthquake Engineering Research (NCEER). Analytical developments and the retrofit phase of the experimental program were also partially supported by the National Institute of Standards and Technology (NIST). The primary purpose of this study is to determine whether these lightly reinforced concrete (LRC) structures need to be retrofitted.

The NCEER experimental program at Cornell University consisted of tests on full-scale beam-column joint specimens and on small-scale model buildings to study the seismic behavior of these structures. These experiments have provided new insights into various damage mechanisms and potential weaknesses. Results of this extensive testing program were used to improve the inelastic dynamic analysis software (IDARC – Inelastic Damage Analysis of Reinforced Concrete [Kunnath, Reinhorn, Lobo, 1992]) and to provide a background for devising repair and retrofit strategies, mitigating seismic hazard, and reducing the risk level to building occupants and owners.

From the experimental results and the preliminary analytical predictions, the development of repair and retrofit methods for these buildings was judged to be necessary. In a NIST report by

El-Borgi, White, and Gergely [1991], various retrofit schemes for reinforced concrete structures were reviewed. This report summarizes an experimental pilot-study on full-scale repaired and retrofitted LRC frame components.

A resin vacuum injection repair technique that is currently used for other types of concrete repair was utilized on an already tested specimen. Also, two local retrofit techniques, using external steel plate attachments, were developed and tested on interior and exterior joints. These methods address buildings in zones of moderate seismicity (about 0.2g maximum ground acceleration). The schemes were also designed to avoid adding significant stiffness to the frame, thus protecting the structure from an increase in demand. The schemes implemented in this study are suggested only for the retrofit of structures where beam-sidesway mechanism are prevalent. To facilitate the evaluation of the upgrades, results of the repaired and retrofitted specimens are shown alongside the results of similar bare specimens.

SECTION 2

EXPERIMENTAL PROGRAM

This section summarizes the relevant details of the earlier NCEER testing program on specimens without retrofit. The same specimen configuration and testing methodology was used for both the bare and the retrofitted beam-column tests. First, the critical details of LRC structures are identified followed by short summaries of the specimen geometry and fabrication details. The loading arrangement and measurement, and test control systems are also discussed.

2.1 Identification of Critical Details

Characteristic reinforcing details widely used in non-seismically detailed building construction in North America were identified through a review of detailing manuals (ACI 315) and design codes (ACI 318) from the past five decades, and in consultation with practicing structural engineers. The following details were found typical and judged to be potentially critical to the safety of LRC structures in an earthquake (figure 2-1).

1. No more than about 2% longitudinal reinforcement in the columns.
2. Lapped splices of column reinforcement located at the maximum moment region just above the construction joint at the floor level.
3. Widely spaced column ties that provide little confinement to the concrete.
4. Little or no transverse reinforcement within the joint region.
5. Discontinuous positive beam reinforcement with a short embedment into the column.
6. Construction joints below and above the beam-column joint.

7. Columns having bending moment capacity close to those of the beams.

2.2 Specimen Geometry and Fabrication Details

The most important specimen dimensions were: 14" x 24" beams with 2-#6 or 2-#8 (continuous or discontinuous) positive bars and with #3 stirrups at 5" spacing, 16" x 16" columns with 1% or 2% reinforcement and #3 ties at 14" and 16" spacing respectively (with the first tie placed 7" and 8" above the joints as specified in past ACI Codes), extra #3 ties at the lower bending point of the offset vertical reinforcement, and 1.5" cover over ties and stirrups. With the exception of four specimens no transverse reinforcement was placed within the joint panel. Nominal material strengths were $f'_c = 3500$ psi and $f_y = 60$ ksi. Some specimens had post-tensioned transverse beam stubs to simulate the presence of lateral confinement from transverse beams framing in from out of plane. No slabs were included in this study.

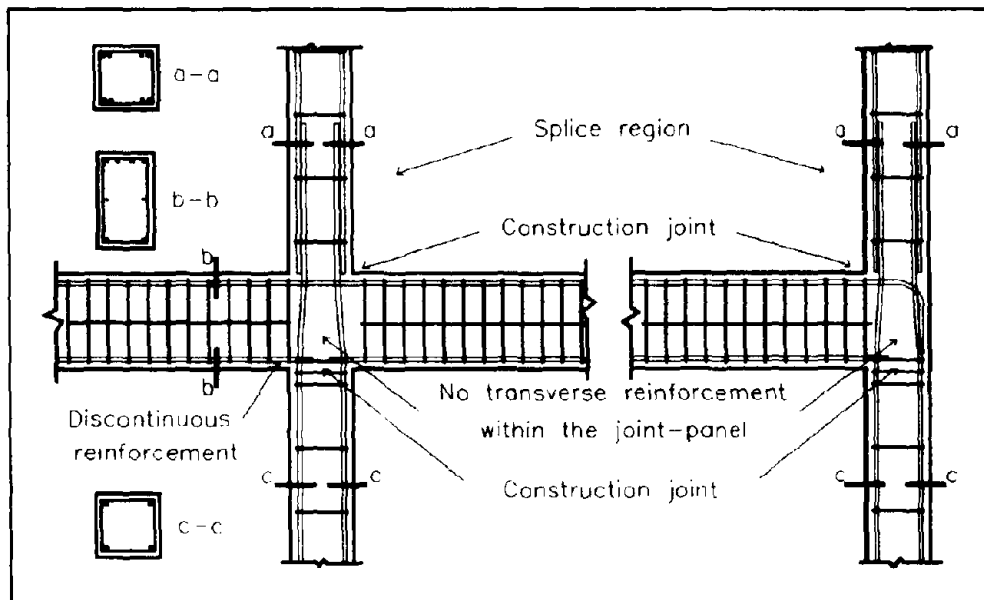


FIGURE 2-1 Elevation View of an Interior and an Exterior Beam-Column Connection

2.3 Loading Arrangement

The following discussion pertains directly to interior joint specimens (a similar procedure was used for exterior specimens).

To simulate seismic action, the specimens were loaded in a computer-controlled testing facility constructed at Cornell. Figure 2-2 shows a photograph of the testing frame with an interior joint specimen in place and ready for testing. Figure 2-3 shows two elevation views of the testing frame, while figure 2-4 shows an idealization of the force and reaction system. Detailed information about the experimental setup is provided in Pessiki, Conley, Bond, Gergely, and White [1988].

The slowly applied reversed cyclic load was controlled by the values of the shear forces acting on the beams, with the "reference" value being 20 kips representing constant dead and service loads on each beam. The preset load-history, demonstrated in figure 2-5, consisted of sets of three cycles applied to the beam ends at paired force levels of 30 and 10 kips, 40 and 0 kips, 50 and -10 kips (negative denotes upward force), and 60 and -20 kips. Low-level cycles (30 and 10 kips) were applied after each third cycle. Loading beyond peak resistance was displacement-controlled by the gradually increasing values of positive beam rotation measured over a distance of 11 inches from the joint. The algebraic sum of the beam forces and the compressive axial force on the top of the column were kept constant throughout the test.

2.4 Measurement and Control Systems

The hydraulic servo-controlled actuators were directed by a control program via MTS Controller System that monitored the independent closed loops in terms of displacement. Forces were measured with load cells at the three (two at exterior joints) actuators and at the top reaction arm. Force and displacement values were displayed at each load increment to provide interaction possibilities for the operator.

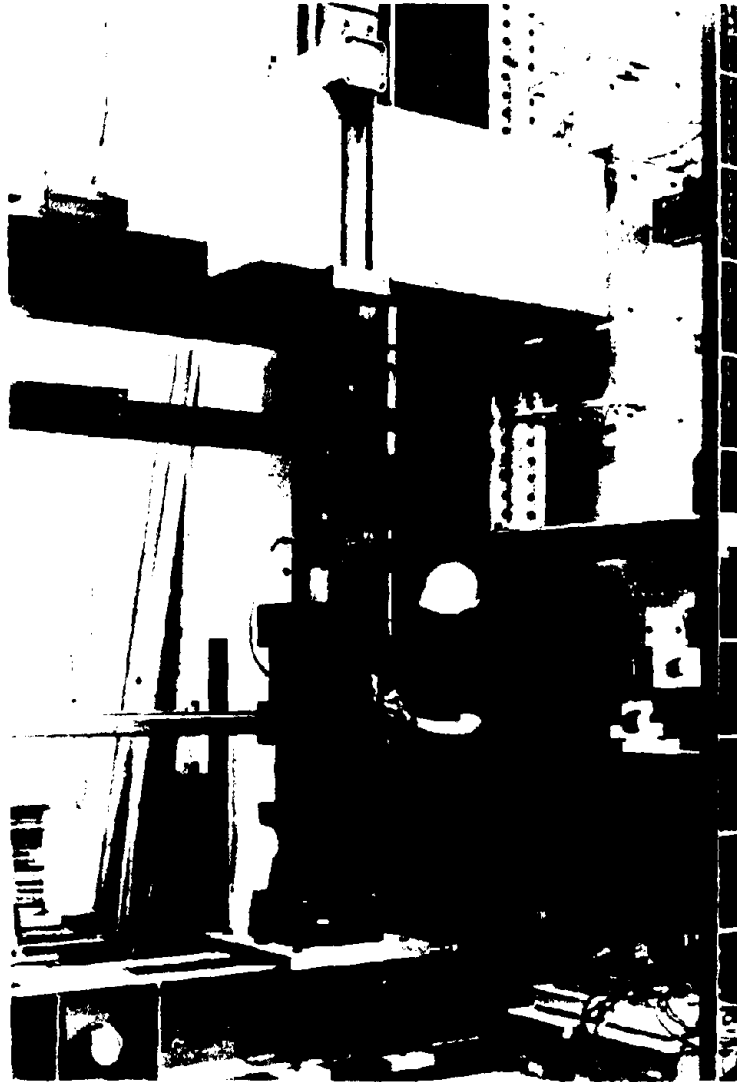


FIGURE 2-2 Photo of the Testing Frame

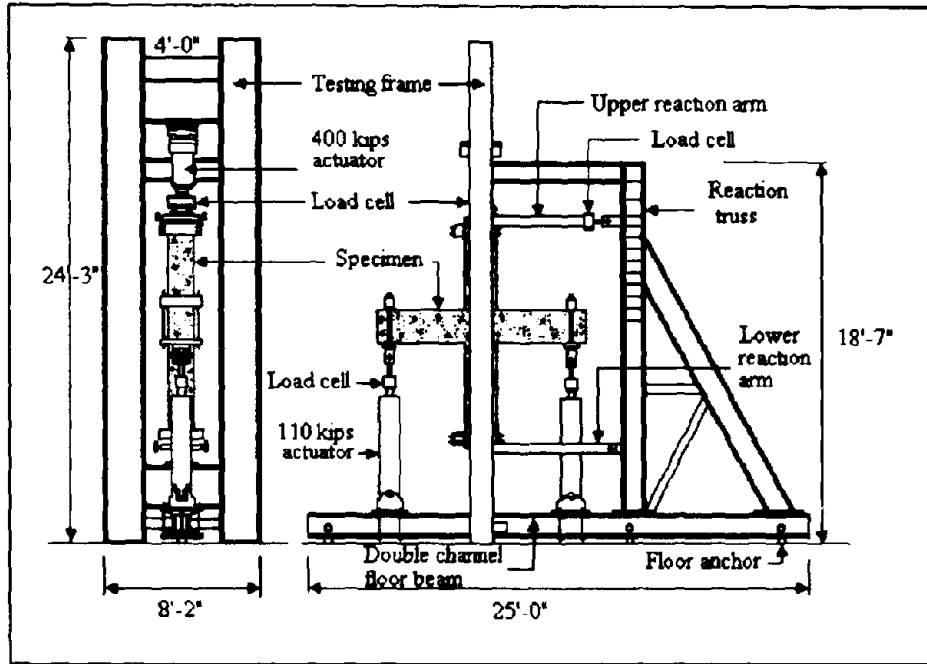


FIGURE 2-3 Two Elevation Views of the Testing Frame (after ref. Pessiki et al. 1988.)

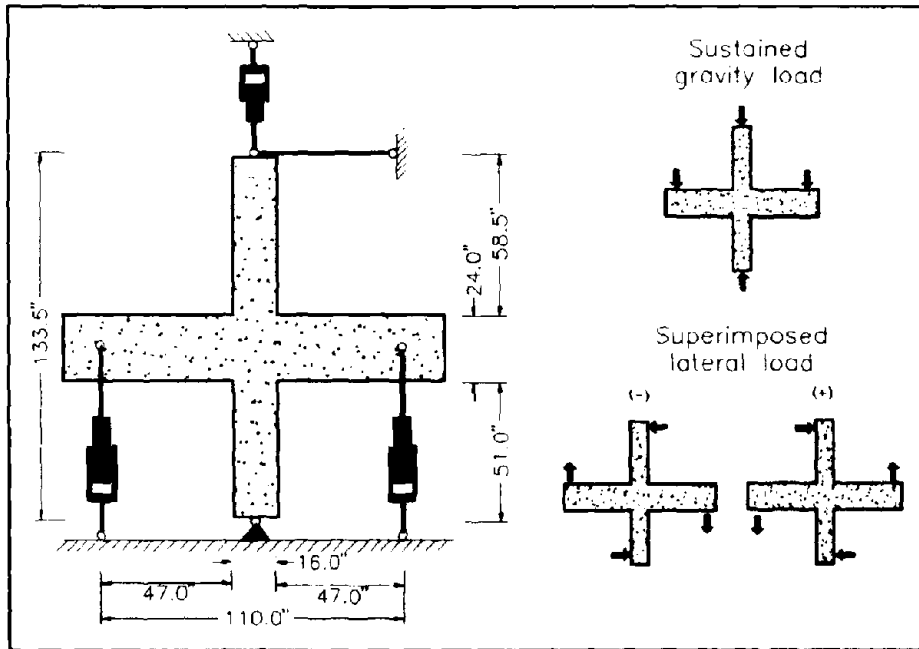


FIGURE 2-4 Idealization of the Force and Reaction System

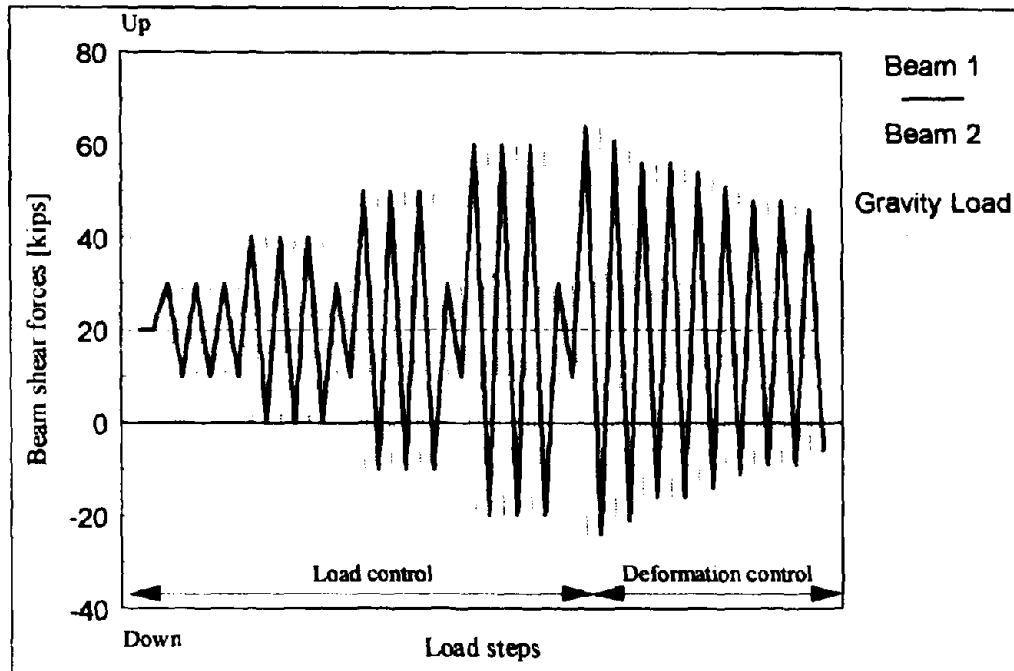


FIGURE 2-5 Typical Load History

Member rotations were computed from measurements made with displacement transducers. These transducers measured relative displacements of points of member cross sections adjacent to the joint over a distance of 11" in the beam(s) and 13.5" in the columns as shown in figure 2-6. Bending moment values shown in the subsequent hysteresis graphs were measured at the interface of the joint-panel and the adjoining beam or column members (unless otherwise noted). Interstory drift was calculated as the total column height multiplied by the amount of rotation the entire specimen must undergo to restore the displaced positions of the end(s) of the beam(s) corresponding to gravity load alone. The retrofitted specimens had additional instrumentation such as strain gages (discussed in Section 5).

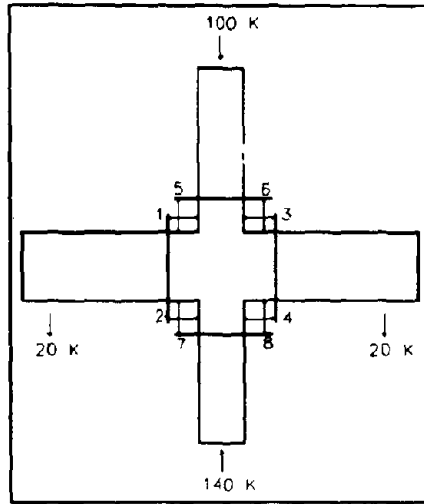


FIGURE 2-6 Arrangement of Instrumentation (DCDTs) for a Typical Interior Specimen with Gravity Load On

SECTION 3

EXPERIMENTALLY OBSERVED BEHAVIOR OF LIGHTLY REINFORCED BEAM-COLUMN JOINTS WITHOUT RETROFIT

This section summarizes the typical behavior and critical aspects of beam-column components tested without any retrofit. Thirty-four specimens have been tested. The detailed results from the tests of the first ten specimens were reported previously by Pessiki, Conley, Gergely, and White [1990], and Beres, Pessiki, White, and Gergely [1991]. Another NCEER report on the remaining results will be published in 1992.

Six interior joint specimens had continuous bottom beam reinforcement through the beam-column joint. These specimens were detailed to investigate the influence of the amount of joint reinforcement and column bar arrangement on joints with spliced and unspliced vertical column rebars. Results are summarized in Section 3.1 based on Pessiki et al. [1990].

Fourteen interior joint specimens had discontinuous positive moment reinforcement extending 6 inches into the columns. Variables studied included the size of embedded reinforcement, column axial force level, amount of reinforcement in the column, transverse confinement of the joint region by perpendicular stub beams, and variation of the concrete strength within the specimen.

Fourteen experiments were conducted on exterior joints to study the effects of column axial force, transverse confinement, amount of reinforcement in the column and ties within the joint panel on the performance of exterior joints.

3.1 Interior Joint Regions with Continuous Bottom Beam Reinforcement

A typical cracking pattern and hysteresis plots are shown in figures 3-1(a,b,c). In all specimens, damage to the column at the splice location was concentrated in a zone below the first column

in the range of 11.8 to 13.6 $\sqrt{f'_c}$ with negligible influence of column bar size and arrangement (as opposed to the maximum allowed 15 $\sqrt{f'_c}$ for seismically designed joints, where f'_c is the compressive strength of the concrete at the joint-panel zone in psi, and this type of joint is classified as type 2, exterior according to ACI-ASCE 352R).

Providing two No. 3 ties in the joint distributed the cracks within the joint, shifted the failure zone from the joint to the splice region, and decreased the rate of strength loss. It did not increase the peak resistance significantly because of the weakness of the lightly confined splice zone.

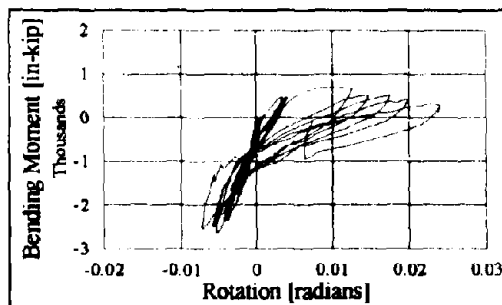
The dominating damage modes were either excessive shear cracking in the joint panel or splice failure above the beam. This points to the prevalence of unfavorable weak column - strong beam type of mechanism.

3.2 Interior Joint Regions with Discontinuous Bottom Beam Reinforcement

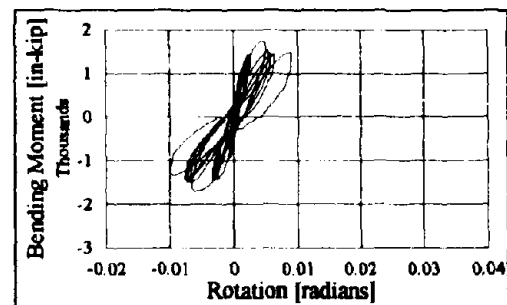
These specimens were constructed with discontinuous bottom beam reinforcement embedded 6 inches into the column. Figures 3-2(a,b) show plots of bending moment versus rotation measured close to the joint of a typical specimen. The individual hysteresis loops are markedly different from those for more thoroughly reinforced joints for several reasons. The hysteresis loops are not symmetrical since (a) the beam reinforcement was not symmetrical; (b) the reversing load cycles produced the superposition of the symmetrical gravity loads and the antisymmetrical loads simulating the lateral action; and (c) the bottom beam reinforcement tended to pull out at higher load levels.

Failure of the typical specimen was initiated by pullout of the discontinuous beam reinforcement from the beam-column joint. At early stages of the test, cracks appeared on the face of the joint in the vicinity of the embedded bars. These cracks progressed as the test continued, eventually merging with diagonal cracks formed also at lower load levels at the top

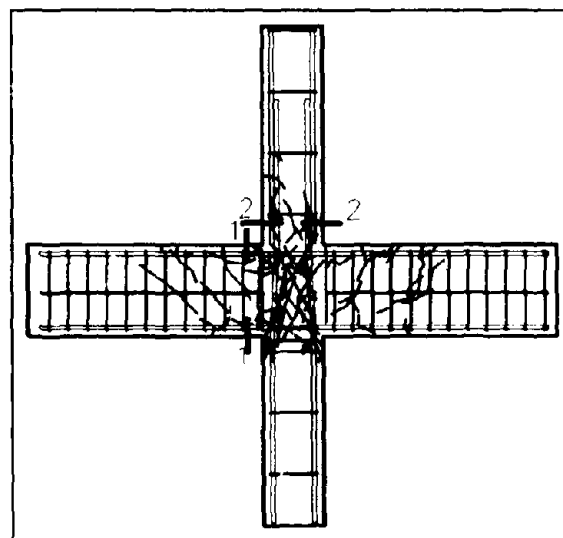
corners of the joint panel due to the downward forces on the beams (figure 3-2(c)). Subsequent cycles gradually opened the diagonal cracks further, causing loss in strength and stiffness. In a few cases, the dominant cracking pattern was different. The major fraction of the total deformation (interstory drift) was attributed to the large rotation caused by vertically propagating cracks at the beam-column interface. Spalling of concrete cover over a distance of 3 to 4 inches above and below the joint, and vertical cracking up to the first tie, occurred in the top column but the splices performed well.



a. Beam Moment-Rotation (Zone 1.)



b. Column Moment-Rotation (Zone 2.)



c. Cracking Pattern

FIGURE 3-2 Typical Interior Joint with Discontinuous Reinforcement

Maximum joint shear stresses at the peak upward forces were 9.1-11.8% up to 40% less than in interior specimens with continuous positive reinforcement. The column axial force was the most significant variable. Specimens loaded with larger axial force (350 kips) exhibited up to 30% increase in load capacity. They had increased energy dissipation capacity and higher overall specimen stiffness in the initial cycles.

Peak strength was reached when the beams were subjected to bending moments of 65 to 90 ft-kips at the beam-column interface. These bending-moment values translate to approximately 42 to 58 ksi stress in the rebars at the bottom of the beams, that was always below the yield stress of the Grade 60 bars. The size of the embedded reinforcement (3/4 and 1 inch diameter) did not significantly influence these values, though the rate of strength loss was larger in specimens with the smaller bars.

Some specimens had transverse beam stubs to simulate the lateral confinement that would be provided by beams framing in perpendicular to the primary frame. Near the bottom of each stub, 50 kips prestressing force was applied over an 8 by 14 inches area to simulate the compressive bending force from gravity load action in a 3-D framing system. The beam stubs produced no marked effect on strength capacity, stiffness degradation or the total energy dissipation. It did cause change in the distribution of damage and energy dissipation among the members framing into the joint. The presence of confinement shifted some of the damage to the column.

3.3 Exterior Joint Regions with Discontinuous Bottom Beam Reinforcement

These specimens were tested to study the behavior of exterior joint region. A load history that simplified comparison with results from the interior joints was applied.

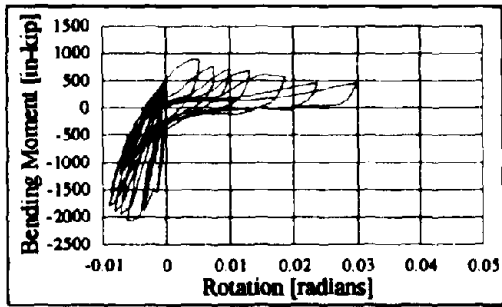
Moment-rotation plots for a typical specimen without transverse beam stubs are given in figures 3-3(a,b). Initial cracks appeared on the face of the joint near the embedded bars during

early load cycles. Under increasing loads, these cracks progressed diagonally across the joint into the splice region. The load carrying capacity dropped suddenly as cracking extended along the entire length of the splice revealing the buckling longitudinal column bars. Additional load cycles induced a large opening of the construction joint above the beam, and drove the cracks along the splice toward the bottom column. The prying action of the bent-down negative beam reinforcement produced full separation of the 2.5–4.0 ft high concrete cover layer opposite the beam (extending from the lower construction joint to the splice region), as shown in figure 3-3(c). In contrast to the interior joints, downward loading on the beams had a major contribution to the failure of the exterior joints.

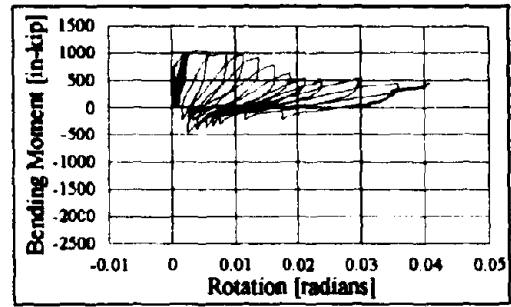
Specimens with transverse beam stubs showed a similar failure mechanism; however, cracking was less severe. Pullout of the bottom beam bars occurred at about the same load (75 to 110 ft-kips bending-moment at the beam) as intensive cracking at the splices. Transverse confinement (either by beam stubs or by two No. 3 ties) increased the peak load capacity by 25–40% and provided a more gradual strength degradation. Specimens tested at the higher level of column axial force (350 kips) showed higher strength, as was the case for interior specimens.

Although the average peak load capacity of exterior joints was about 20% higher than that of interior joints, strength degradation of exterior joints was more rapid because of higher levels of damage to the splice region. Further analysis of data will lead to firm conclusions about the behavior of joint regions with discontinuous embedded reinforcement.

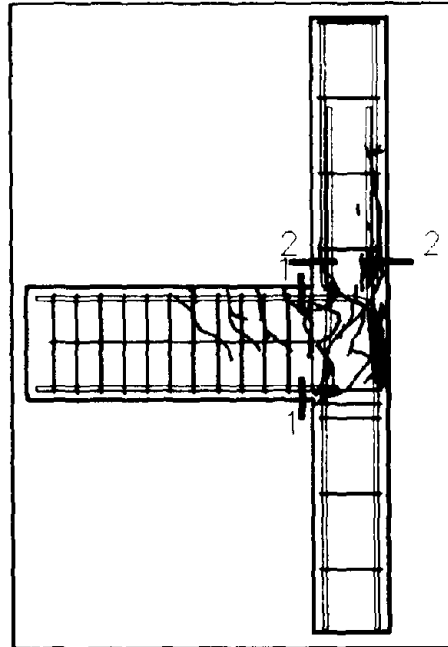
In summary, failures occurred by a combination of excessive diagonal shear cracking followed by splice failure in the top column, spalling of the concrete cover due to the prying action of the bent-down negative beam reinforcement, and to a smaller extent, pullout of the embedded positive beam reinforcement.



a. Beam Moment-Rotation (Zone 1.)



b. Column Moment-Rotation (Zone 2.)



c. Cracking Pattern

FIGURE 3-3 Typical Exterior Joint with Discontinuous Reinforcement

SECTION 4

SEISMIC REPAIR SCHEME

4.1 Introduction

The extensive testing program summarized in Sections 2 and 3 made damaged specimens available for repair and retesting. This section describes one repair method tried at Cornell.

With the help of Balvac Incorporated, an experiment was performed to investigate the effectiveness of a resin injection repair method used on a severely cracked beam-column joint region. There has been very little research in this field. In a recent paper [French, Thorp, and Tsai, 1990], it was shown that epoxy repairs were highly successful in similar specimens designed with reinforcement continuous through the joint, as is used in modern seismic detailing. Both the strength and the stiffness of the damaged specimens were restored to near the original values in specimens repaired by either the pressure injection technique or the vacuum impregnation technique, and energy dissipation capabilities of both repaired specimens during critical load cycles were also excellent. There was substantial bond damage done to the specimens in the beam-column joint region during the higher level of loading, but certainly not as severe as in the specimen described in this report. Several researchers [Bertero, and Popov, 1977], [Corazao, and Durrani, 1989] indicated that pressure injection was not able to fully restore the bond between the embedded rebars and the concrete because of inadequate penetration.

4.2 Evaluation of Test Results and Comparisons with Non-repaired Specimens

The repair was carried out on a previously tested specimen, referred to here as I-11. A detailed description of the behavior of the class of specimens (interior joints with discontinuous reinforcement) represented by I-11 is included in Section 3.2. The test on the repaired

4.2.1 Repair Scheme

Resin impregnation by a special vacuum technology was used to bind the cracked concrete surfaces to each other to improve the structural integrity and the load capacity of the specimen. The repair work itself was done by Balvac using their patented technology to best simulate the actual construction practice. There was no previous experience on their part with applications related to seismic resistance.

Vacuum impregnation was chosen versus the conventional pressure injection technique because of several potential advantages of the former:

- Deeper penetration of the resin, and more complete filling of the interconnected crack system to eliminate pressure pockets and dead end cracks.
- Lower limits on the viscosity of the materials used.
- Less chance to promote further damage by avoiding positive pressure buildup.

The goal of the vacuum impregnation technology is to provide better bonding capacity. To achieve this goal, first the loose concrete pieces were removed from the damaged surface. Then the voids were filled with a high early strength repair mortar (SIKATOP 122), as shown in fig. 4-2a. This patching work was necessary at the middle of the joint, where approximately 1-1.5 inch thick, 10 inch diameter circular shaped piece of concrete cover was missing on both sides, and at the corners of the joint, especially around the embedment region where smaller pieces of the cover spalled away.

The repaired joint region was sealed by CELTITE 21-20 POLYGEL (see figs. 4-2b,c), followed by the vacuum injection of the BALVAC 1173 methyl-methacrylate resin. Though only those cracks which were effectively connected to the joint region were sealed and impregnated, a large quantity (about 3 gallons) of resin was used. Finishing the repair, the

sealing gel was ground off from the surface to make the crack pattern visible during the test. The applied repair method did not change the original geometry of the specimen.



a. Initial Layer of Patching Mortar in Place



b. Preparing for Resin Injection



c. Resin injection Process

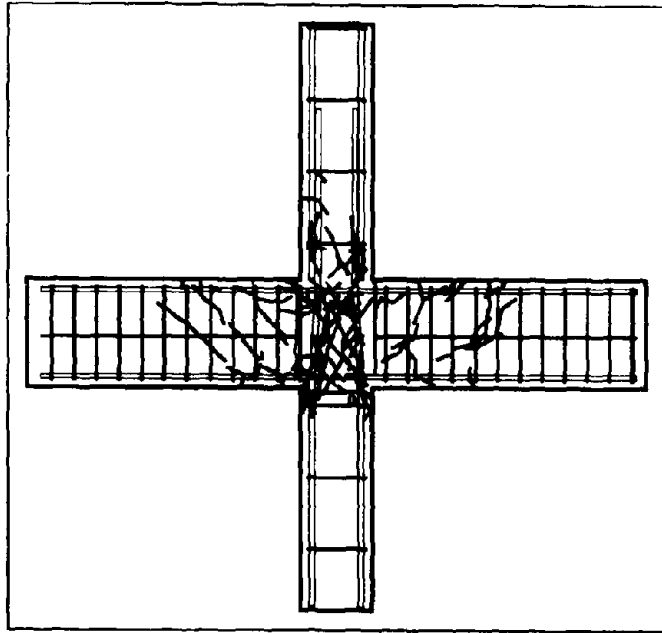
FIGURE 4-2 Implementation of the Repair

4.2.2 General Behavior of Repaired Specimen and Damage Progress

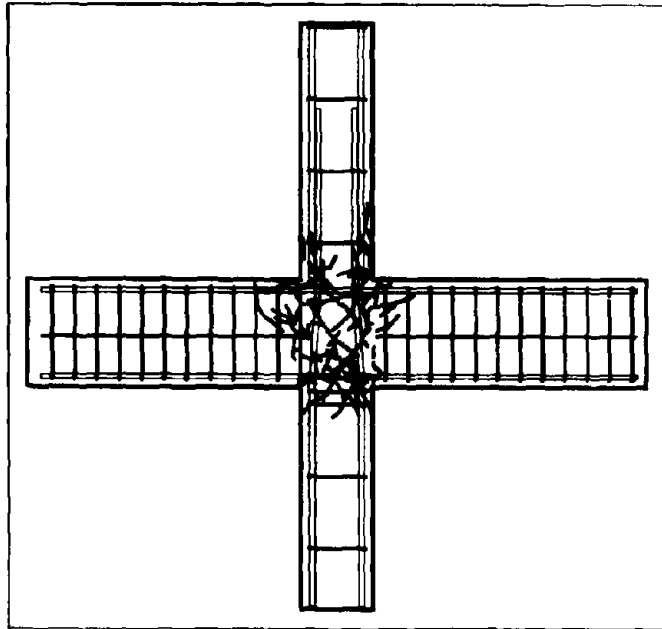
At the application of the gravity load and the preload (which is a low force level on the specimen simulating pre-earthquake live load action), no visible cracking of the repaired region was observed. During these and other low level cycles (before applying the peak loads), relatively large beam rotations and lateral displacements were experienced compared to the virgin specimen. This was because of the reduced stiffness of the non-repaired cracked regions (some major cracks that occurred away from the joint panel at high level cycles were not repaired) and the possibly lower stiffness of the repaired zones.

At low force level cycles, cracks developed between the patching mortar and the original concrete at the joint surface. Although these cracks (see figure 4-3(a,b)) became increasingly apparent during the cycling, the first spalling of the patching mortar occurred at a relatively high beam rotation value of +0.0175 radian. Additional cycles caused extensive spalling at the concrete cover of the middle joint region and around the corners, especially at the adjacent column surfaces. After removing the loose pieces, the same main diagonal cracks as in the original specimen were found in the joint, and the concrete seemed to be extensively deteriorated as shown in figure 4-4. Compared to the crack pattern of the original specimen, new vertical cracks were found in the upper column extending from the joint beyond the first stirrup above the joint.

The failure of the specimen to maintain load capacity was attributed to the pullout of the embedded bottom rebars of the beams in both the original and repaired specimens. The repaired specimen reached a value of about 72% of the peak column shear capacity of the original specimen. Heavy concrete damage was visible around the embedment zone and the main diagonal cracks went through this region as well, as can be seen in figure 4-4.



a. Specimen I-11



b. Specimen REP I-11

FIGURE 4-3 Cracking Patterns



FIGURE 4-4 Photo Taken After the Test

After the test, the loose concrete pieces were removed. In most cases it was impossible to tell where the original cracklines were because of the lack of visible color differences at the joint, except for some thin resin layers around the vertical rebars. Much of the concrete seemed to be "soaked" by the resin, having a dark gray color. Some parts of the concrete underwent a slight

color change, and the surface gave the general impression that the resin might not have uniformly cured.

4.2.3 Specimen Strength and Interstory Drift

Figures 4-5(a,b) show the relation between the shear force acting at the midheight of the column and the interstory drift, i.e. the relative lateral displacement of the adjacent floors, for the original and repaired specimens. The magnitude of story-drift can be related to the total damage of the structure. When the virgin specimen was loaded up to 3.8% interstory drift during the final cycle it experienced serious deterioration. The repair did restore about 72% of the column shear force capacity, with load levels remaining constant for 5 cycles.

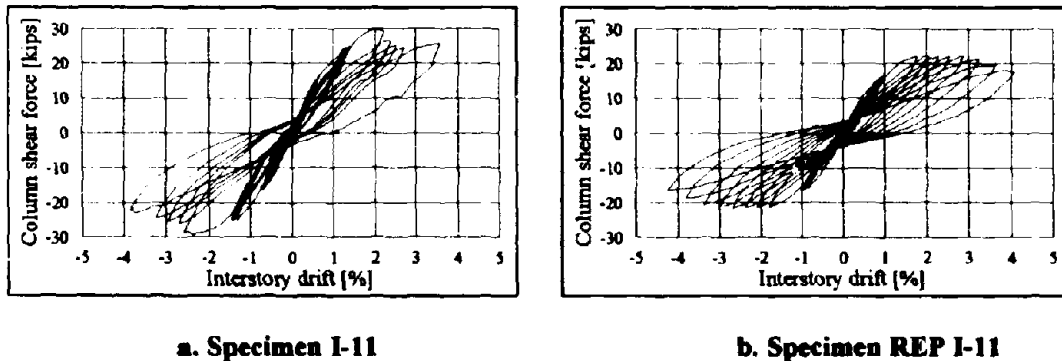
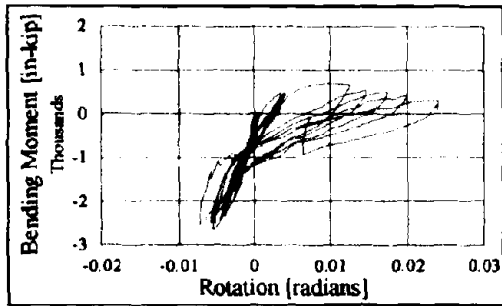


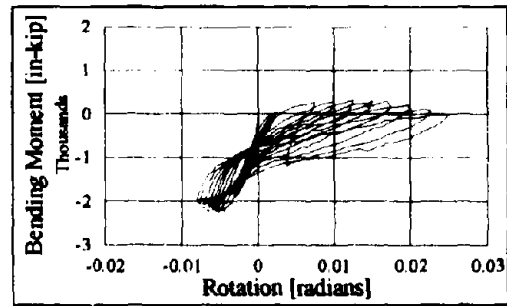
FIGURE 4-5 Column Shear Force Versus Interstory Drift Before and After Repair

The bending moment - rotation relations for the beam regions adjacent to the joint are shown in figures 4-6(a-d). The moment-rotation plots are of particular importance, because the failures of both specimens were attributed to the pullout of the embedded rebars at the bottom of the beams. From the bending moment - rotation plots it can be seen that in spite of the fact that only about 40% of the positive bending moment capacity of the original specimen was reached, this capacity was maintained through a relatively large rotation value of more than

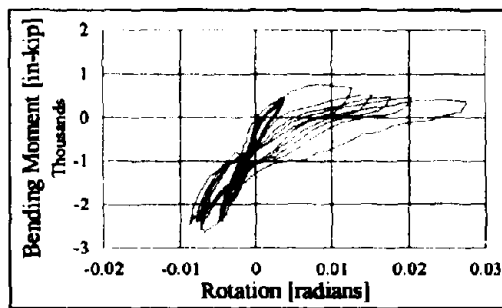
+0.02 radian (see the positive moment and positive rotation region, because this part of the hysteretic action is related closely to the pullout action).



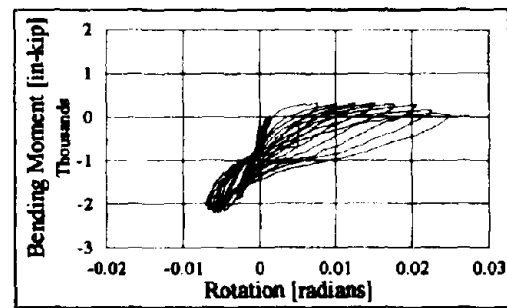
a. Specimen I-11 Beam #1



b. Specimen REP I-11 Beam #1



c. Specimen I-11 Beam #2



d. Specimen REP I-11 Beam #2

FIGURE 4-6 Bending Moment Versus Rotation in Beams Before and After Repair

4.2.4 Specimen Stiffness

Stiffness degradation is illustrated by a plot of the specimen stiffness versus the average of the maximum absolute values of the positive and negative interstory drifts (figure 4-7). The specimen stiffness corresponds to the peak-to-peak slope of each cycle in the column shear versus interstory drift. Since only a part of the cracked zones were repaired, the initial stiffness of REP I-11 was about 25% less than that of the virgin specimen. The repair scheme resulted in a similar degradation path with convergence at high deformations.

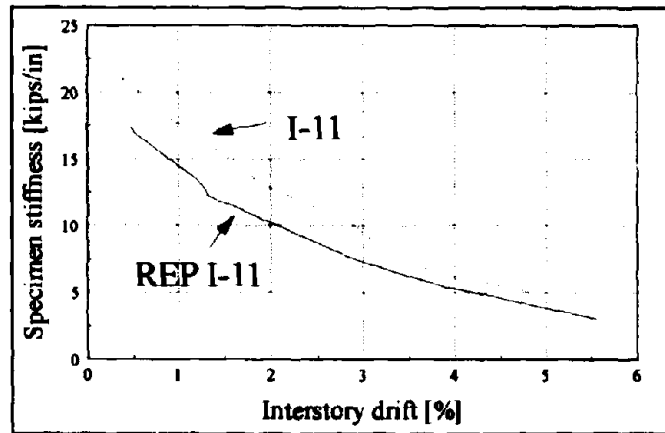


FIGURE 4-7 Stiffness vs. Maximum Interstory Drift Before and After Repair

4.2.5 Energy Dissipation

Energy dissipation is represented by a plot of the cumulative dissipated energy versus the average of the absolute values of the maximum positive and negative interstory drifts (figure 4-8). The cumulative dissipated energy was computed by summing the area enclosed within the column shear versus average interstory drift. This is an approximation, because frictional losses induced are not accounted for during the test.

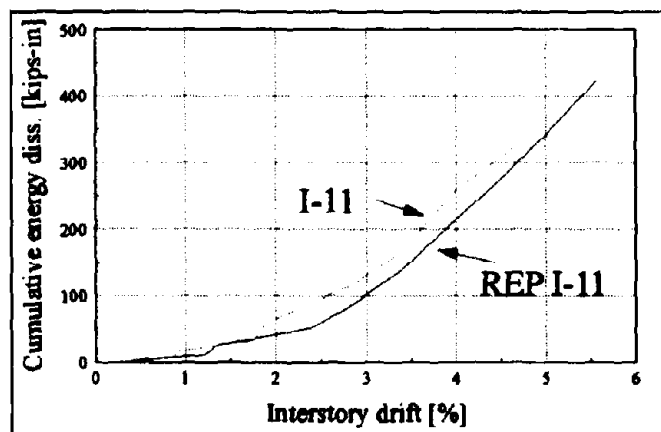


FIGURE 4-8 Cumulative Energy Dissipation vs. Interstory Drift Before and After Repair

Figure 4-8 shows that energy dissipation was almost identical for the repaired and the virgin specimens. The slightly higher cumulative energy values for I-11 are attributed to the fact that only cracks close to the joint-panel zone were filled with resin and few new cracks developed outside this region during the retest. Beyond 2% drift, substantial cracking and loss of stiffness occurred in both cases. This caused an increase in the energy dissipation rate.

4.3 Summary

The applicability of a modern repair method was investigated for potential use in post-earthquake rehabilitation work. Although the results of this test showed that the load bearing capacity of the joint was not fully restored, the energy dissipation capability and stiffness degradation of the specimen were promising. The following possibilities might be considered for further research.

- A. The repair reported here was made on a heavily damaged specimen. It is quite possible that in cases of relatively minor damage to the specimen, this repair technology might work much more effectively. Previous tests at Cornell showed that in cases of two-way frames (specimens with transverse beam stubs at both sides), the deterioration of the joints can be much less. It is suggested that repair be done on a specimen that is not loaded to such high damage levels. Another worthwhile experiment would be to construct specimens with continuous rebars at the bottom of the beams.
- B. Although the test data about the compressive and tensile strength of the repair resin provided by Balvac showed the material to have excellent strength properties, the bond characteristics may need further improvement. To achieve effective structural repair on this type of reinforced concrete structure, the bond properties of the resin (both to concrete and to reinforcement) must be sufficient. The bond and tensile characteristics should be studied as a function of curing time and environmental conditions (temperature, humidity) as well. To enhance the bond performance of the embedded

discontinuous reinforcement, small scale pullout tests might be useful in optimizing the resin choice.

- C. Because of the rather severe degradation of the concrete and the size of cracks, it is suggested that the use of a resin of "heavier" consistency be considered. This suggestion is based on the appearance of bond lines at cracks in the repaired specimen (observed after the retest had been completed), which indicated some tendency of resin penetration into the concrete and starved bond lines at the cracks.
- D. Repair of the bond between concrete and reinforcing steel is a very difficult task and may require a different resin from that used to repair cracks in the concrete. It might be possible to drill in from the beam surface to the embedded reinforcement and inject resin more directly into the disturbed interface between the concrete and the reinforcement.
- E. It might be worthwhile to consider using this repair technique in combination with other methods (e.g., the bonded plate method) depending on the damage to the given member of the structure.

SECTION 5

SEISMIC RETROFIT SCHEMES

5.1 Introduction

From the experiments described in Sections 2 and 3 and the preliminary seismic analyses of the selected LRC buildings, described in the previous NIST report [El-Borgi, White, and Gergely, 1991], it was possible to identify some potential weaknesses in such structures. The development of simple retrofit methods for these buildings was judged to be necessary. In the above reference, various retrofit schemes were also reviewed. After consultation with practicing engineers, a local retrofit technique consisting of external steel plate attachments was chosen. Other methods are currently being investigated under NCEER sponsorship [Corazao, and Durrani, 1989, Choudhuri, Mander, and Reinhorn, 1992, Bracci, Reinhorn, and Mander, 1992].

The experimental results presented in Section 3 showed various damage modes depending on the parameters examined. Consequently, different external plate configurations were considered for one interior joint and one exterior joint. The parameters of the retrofitted specimens were chosen from those examined in the bare component testing program based on the highest likelihood of their occurrence in existing buildings.

Two schemes were used to retrofit beam-column components of LRC frame buildings in zones of moderate seismicity. Both schemes are practical and inexpensive, representing a lower-end retrofit as opposed to the full steel-jacketing scheme used at U. Texas [Estrada, 1990] for higher seismicity zones. The first scheme was used for typical interior joints with discontinuous bottom beam reinforcement, and the other for exterior joints with discontinuous bottom reinforcement and with a smaller axial load.

The objectives of these upgrades are briefly summarized in the following sections. For the purpose of comparison, the selected experimental results are shown with those of corresponding bare joint components having similar details.

5.2 Interior Joint

5.2.1 Retrofit Scheme

The main objective of this scheme was to delay the effects of the early pullout of the embedded positive beam reinforcement. Although pullout would be favorable when it causes beam hinging, but as the experiments showed, the early debonding of the embedded positive beam rebars triggered brittle shear failure in the joint panel and resulted in high flexibility of the beam-column specimen. The retrofit was done by providing continuity of this reinforcement through the use of external steel plate attachments. Prevention of pullout would thus delay damage in the joint panel and postpone the loss of stiffness and strength, thereby also reducing the second order ($P-\Delta$) effects. This retrofit scheme was chosen with the understanding that pullout might be beneficial for certain buildings, if damage to the column is limited. Simultaneous upgrade of the column may be warranted for many LRC structures that have column flexural strength capacity only slightly exceeding that of the beams. Therefore, global analysis of the non-retrofitted structure may be necessary to prevent the formation of undesirable weak-column (soft-story) mechanism.

As shown in figures 5-1 and 5-4, attachments consisted of two steel channel sections bolted to the underside of the beams. The channel sections were connected by two steel tie-bars (1" by 1/2" flat stock) running alongside the column. All steel members used were A36 grade. A 1/2 inch thick mortar layer was placed between the steel plates and the concrete surfaces to provide more ductile behavior of the anchor bolts in shear. Adhesive anchor bolts (Williams S6S-ACA, 5/8" diameter, 5" embedment length), 6 at each beam, were used to attach the steel

The dimensions of the steel elements were based on approximate calculations. The size of the connecting tie-bars (nominal yield strength of 18 kips each) was chosen such that both bars would be capable of carrying the largest load (about 20 kips) experienced by the individual embedded positive beam reinforcement in a bare specimen.

To simulate retrofit in an actual building, the beams were preloaded with gravity loads of 20 kips on each actuator. This was followed by a low-level cycle of 15 kips and 25 kips peak loads to simulate the effect of the changing occupancy load. The steel tie-bars were then welded onto the plates with gravity loads applied on the beams.

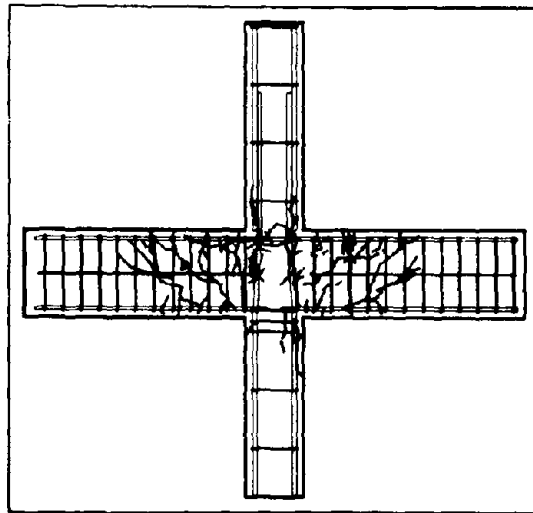
This retrofit scheme could also be done in a three-dimensional configuration of beams and columns.

In this section, the experimental findings of the retrofitted specimen (RI-1) are summarized and compared with a previously tested bare specimen (I-16). Several topics will be addressed including damage progress, specimen strength, interstory drift, specimen stiffness, and energy dissipation.

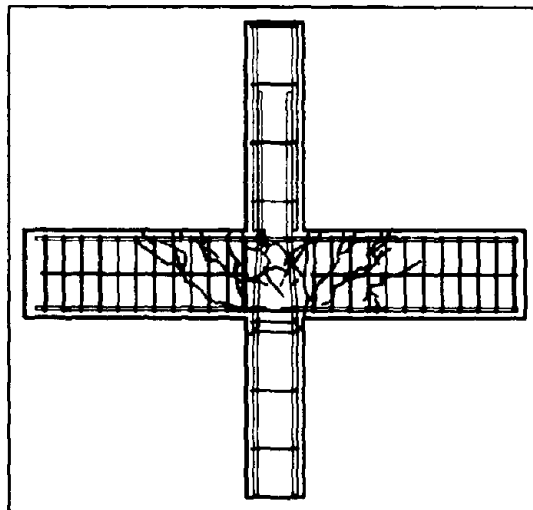
Figure 5-2 shows the reinforcement details and dimensions for both the bare and the retrofitted specimens. The characteristic parameters of both specimens were:

- 4-#10 spliced rebars in the column
- 2-#8 and 2-#6 continuous negative rebars in the beam
- 2-#8 embedded positive rebars in the beam
- 350 kips axial force on the top of the column
- Transverse beam stub confinement
- No ties within the joint

cracking patterns for both bare (I-16) and retrofitted (RI-1) specimens are shown in figures 5-3(a,b). After completion of the test (figure 5-4), no significant permanent deformations were noticed on the retrofitted specimen.



a. Specimen I-16



b. Specimen RI-1

FIGURE 5-3 Cracking Patterns (interior)

5.2.2.2 Specimen Strength and Interstory Drift

The specimen behavior can be characterized best by plots of the column shear force versus interstory drift (figure 5-5(a,b)). Since the concrete strength of the joint governed the total capacity, figures 5-6, 5-8 and 5-9 were normalized by $\sqrt{f'_c}$ (f'_c is the measured compressive strength of the concrete in the joint-panel and the beams at the time of testing. The f'_c values were 3600 and 2660 psi for specimens I-16 and RI-1 respectively). Following the low-level elastic cycles, the specimens were loaded at each cycle to their peak load capacities. By connecting the peak points of each hysteresis loop, column shear capacity envelopes were created. Figure 5-6 shows these envelopes for both the non-retrofitted and the retrofitted specimens. The form of the individual hysteresis loops are very similar (figure 5-5), except for slightly more pinching in the non-retrofitted specimen which exhibited more slip of the embedded rebars.

Figure 5-6 indicates a slight increase of about 20% in the peak strength. The strength deterioration was substantially delayed in the retrofitted specimen doubling the ductility.

A test done on an bare interior joint with continuous reinforcement (I-02 reported by Pessiki, Conley, Gergely, and White [1990]) having similar parameters to the retrofitted specimen showed closely matching strength results and deterioration mode.

5.2.2.3 Stresses in the Connecting Tie-bars

Strain gages were installed on the connecting tie-bars of the retrofitted specimen. Three gages were placed on each steel bar (on the top, bottom, and midheight at the middle cross-section) to monitor the total force and the distribution of longitudinal normal stresses. As mentioned earlier, the bars were welded onto the channel sections while the specimen was loaded with gravity forces. However, to attach all the instrumentation, the specimen had to be unloaded after welding. Consequently, during the testing, the application of the initial gravity load

resulted in a measured compressive strain in the tie-bars. This compressive strain translates to about 5 ksi stress as shown in figure 5-7. In a real application, this initial shift would not happen.

During the test, there was no significant increase in compressive stress. The average maximum increase in tensile stress was about 33 ksi. This value is close to the nominal yield capacity of the A36 steel. The strain gage measurements showed about 15–25% lower peak tensile stresses at the bottom of the tie-bars compared to the top. At maximum load the anchor bolts were subjected to an average shear force of 5.5 kips (that is about 50% of their ultimate strength) without any noticeable damage.



FIGURE 5-4 Photo Taken After the Test (interior)

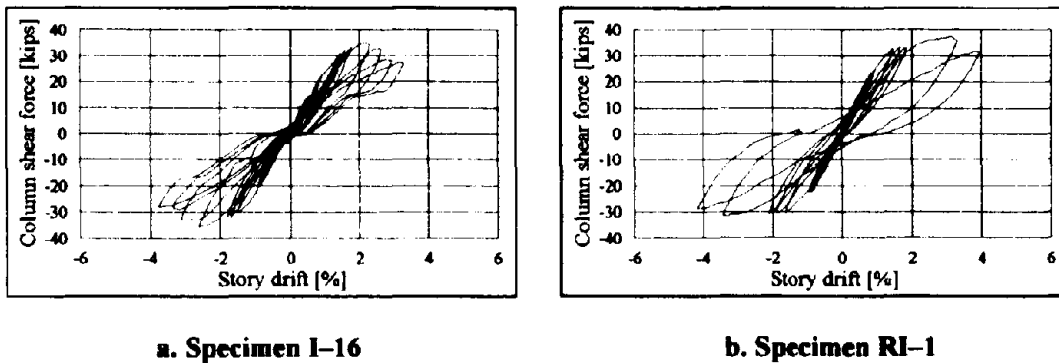


FIGURE 5-5 Column Shear Force Versus Interstory Drift (interior)

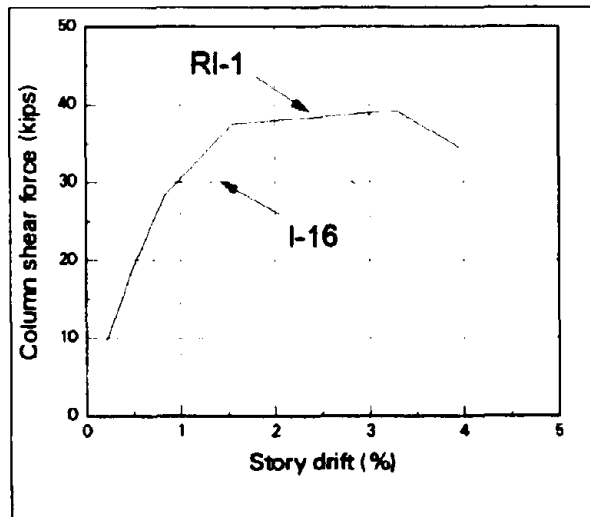


FIGURE 5-6 Column Shear Force Versus Interstory Drift Envelopes (interior)

5.2.2.4 Specimen Stiffness

Stiffness degradation is illustrated by a plot of the specimen stiffness versus the average of the absolute maximum values of the positive and negative interstory drifts (figure 5-8). The specimen stiffness corresponds to the peak-to-peak slope of each cycle in the column shear versus interstory drift. The retrofit scheme resulted in 10 to 20% increase in stiffness. The rates of stiffness degradation for both specimens were similar.

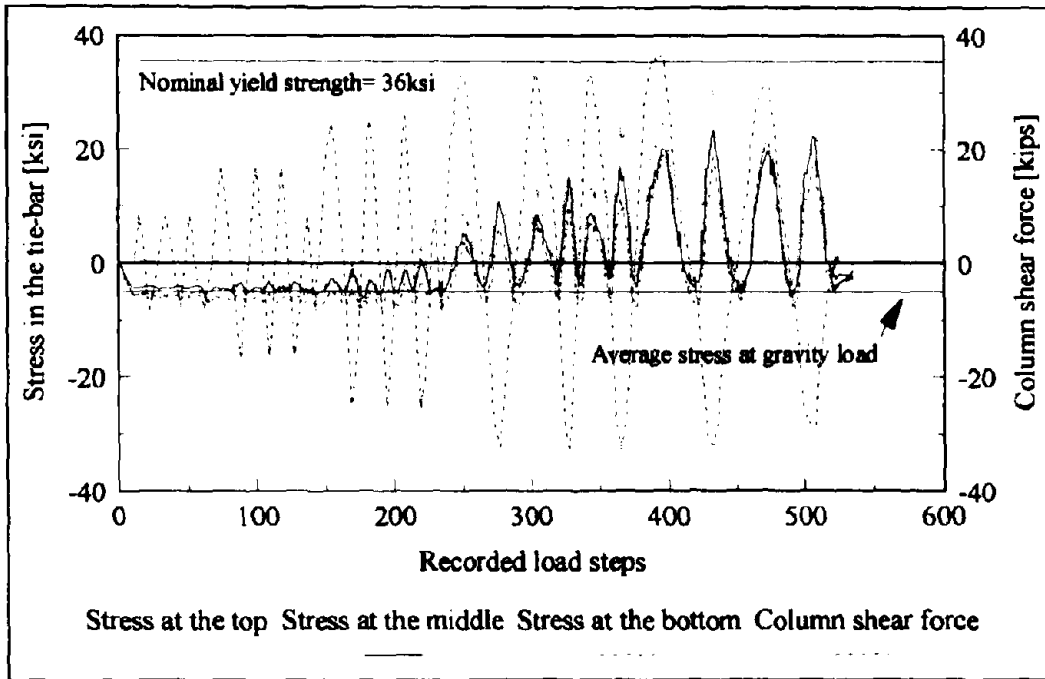


FIGURE 5-7 Longitudinal Stress in the Tie-bars (interior)

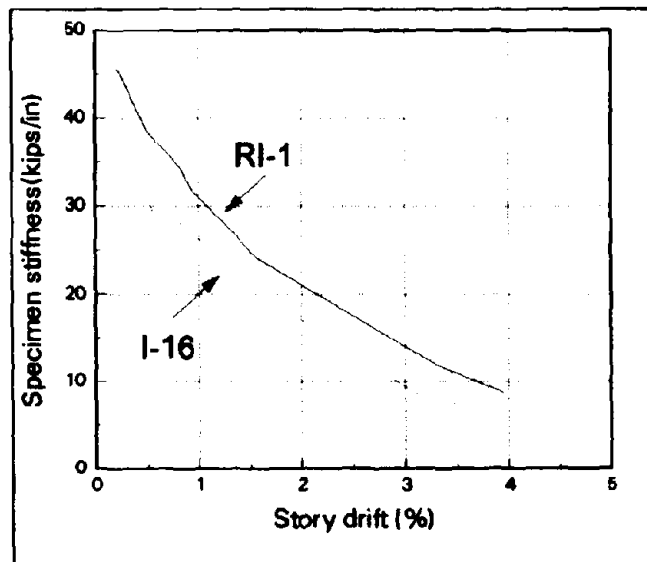


FIGURE 5-8 Stiffness vs. Maximum Interstory Drift (interior)

5.2.2.5 Energy Dissipation

Energy dissipation due to the extensive inelastic action within and near the joint-panel is represented by a plot of the cumulative dissipated energy versus the average of the absolute values of the maximum positive and negative interstory drifts (figure 5-9). The cumulative dissipated energy was computed by summing the area enclosed within the column shear versus average interstory drift. This is an approximation because of frictional losses induced during the test.

Figure 5-9 shows that energy dissipation was almost identical for the retrofitted and non-retrofitted specimens. Although the tie-bars remained elastic and the embedment zone intact, damage was transferred to other parts of the joint because the close hierarchy of weaknesses. Beyond 2% drift, substantial cracking and loss of stiffness occurred in both cases. This caused an increase in the energy dissipation rate.

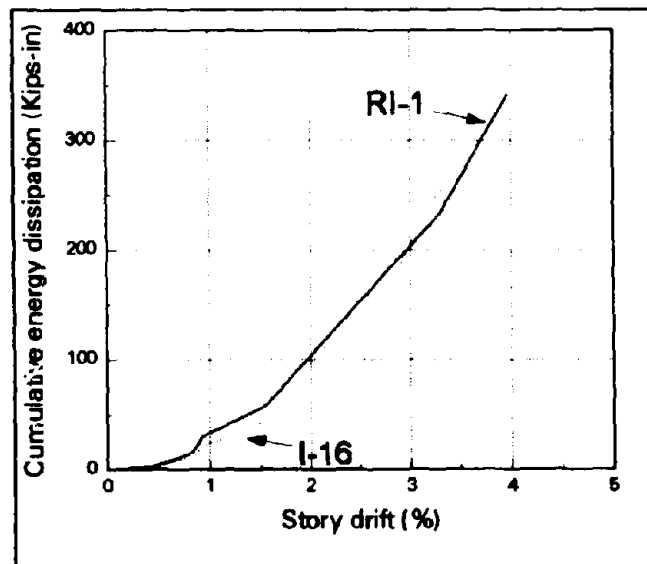


FIGURE 5-9 Cumulative Energy Dissipation vs. Interstory Drift (interior)

5.2.3 Summary

A simple, lowcost retrofit method was used on an interior beam-to-column joint specimen to eliminate positive reinforcement pullout as the critical mechanism controlling joint region capacity. This experiment showed that with minimum effort, significant changes can be made to the behavior of this type of specimen.

The damage mechanism was altered markedly by preventing the pullout of the positive beam reinforcement. Most of the damage was transferred from the embedment zone to other parts of the joint panel, and to smaller extent to the top of the beam and to the upper construction joint. The column shear capacity increased by 20% with a slower rate of degradation due to the prevention of the very brittle pull-out type of damage. Although pullout did not occur, the stiffness characteristics changed insignificantly (10–20% increase, with the same degradation rate), while the energy dissipation remained the same. Because of the close hierarchy of different critical damage mechanisms at the joint region, only a modest capacity increase was achieved. The small increase in stiffness suggests that second order analysis might also be needed for the retrofitted structure.

5.3 Exterior Joint

5.3.1 Retrofit Scheme

The main objective of this scheme was to try to force the flexural hinges to form in the beam but not in the columns, to avoid the occurrence of the soft-story collapse mechanism. The other objectives were to add more confinement to the joint panel, to avoid any splice failure in the top column and to enhance the energy dissipation capacity of the joint. This was done by external steel plates attached along the opposite faces of the upper and lower columns (figures 5-10 and 5-13). An additional consideration in choosing this configuration was the least disturbance of the building facade.

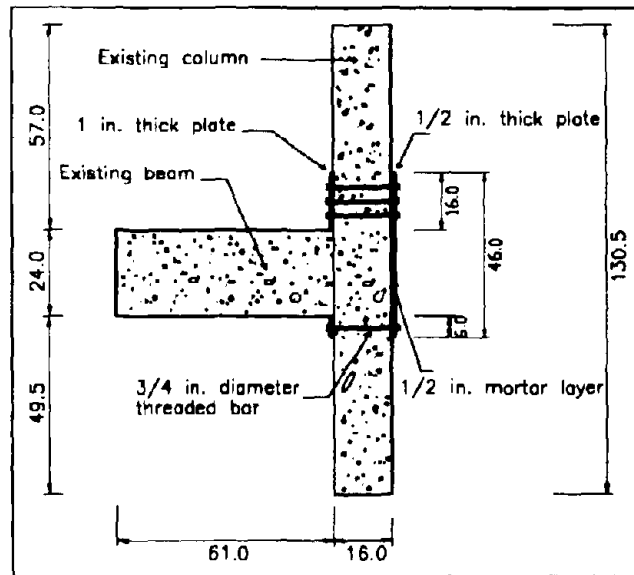


FIGURE 5-10 Retrofit Configuration (exterior)

As shown in figure 5-10, the steel plates were not bolted to the concrete but simply connected with threaded bars. A longer plate was used in the upper column because of the presence of the splice. A 1/2 inch thick film of grout was first placed between each plate and the concrete surface to provide a uniform bearing surface. The threaded rods were then tightened resulting in substantial confining stresses applied to the top and bottom columns.

5.3.2 Evaluation of Test Results and Comparisons with Non-retrofitted Specimens

In this section the experimental findings of the retrofitted specimen (RE-1) are summarized. To help evaluate the results, they are shown alongside the results of a similar bare specimen (E-07). Several topics will be addressed including damage progress, specimen strength, interstory drift, specimen stiffness, and energy dissipation.

Figure 5-11 shows the reinforcement details and dimensions for both the bare and the retrofitted specimens. The characteristic parameters of both specimens were the following:

- 4-#10 spliced rebars in the column

- 2-#6 and 2-#8 bent-down negative rebars in the beam
- 2-#6 embedded positive rebars in the beam
- 100 kips axial force on the top of the column
- No transverse beam stub confinement
- No ties within the joint

5.3.2.1 General Behavior and Damage Progress

The deterioration mode for exterior joints with discontinuous positive beam reinforcement and 2% column longitudinal reinforcement was dominated by damage in the column. Excessive diagonal shear cracking developed in the joint panel zone followed by splice failure in the top column. The prying action of the bent-down negative beam reinforcement resulted in spalling of the concrete cover.

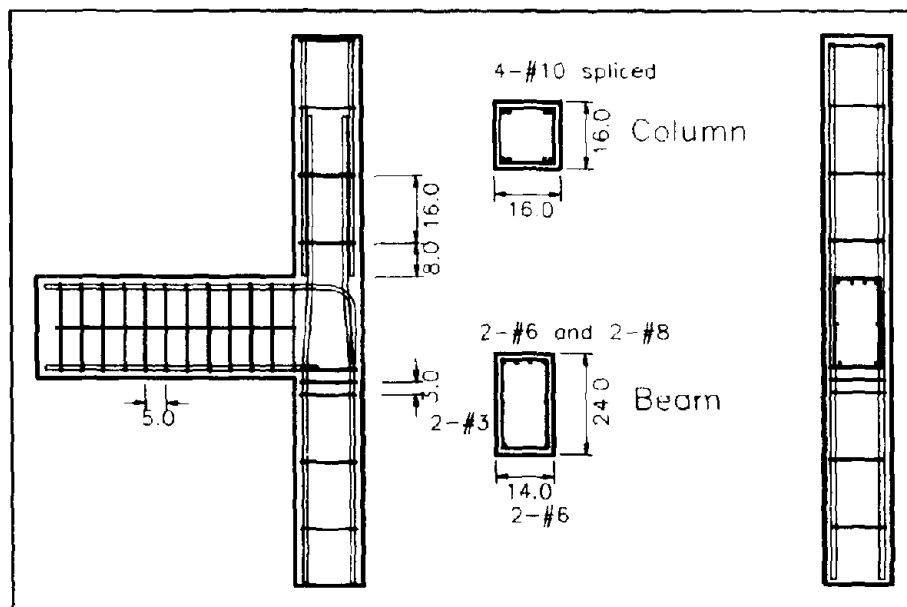


FIGURE 5-11 Specimen Reinforcement and Dimensions (exterior)

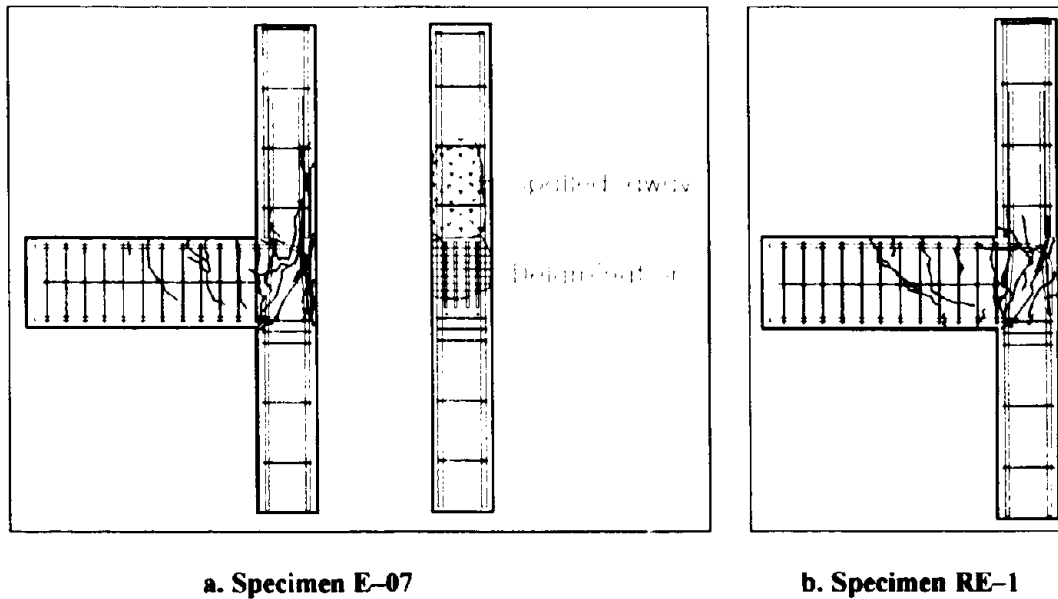


FIGURE 5-12 Cracking Patterns (exterior)

The implemented retrofit scheme markedly changed the damage pattern, especially toward the end of the test. Initial cracks developed similarly to the bare specimen. However, no major opening of the diagonal cracks were observed. Subsequent cycles caused few extensions of these cracks beyond the upper construction joint into the splice region. Cracks in that zone were effectively arrested by the steel plate confinement. Spalling of the concrete cover opposite to the beam was entirely prevented by the back side steel plate resulting in significantly less damage in the joint panel zone. At the final cycles, a major vertical crack developed in the joint panel close to the beam, resulting in the formation of a flexural hinge. This was followed by pullout of the positive beam reinforcement. Final cracking patterns for both bare (E-07) and retrofitted (RE-1) specimens are shown in figure 5-12(a,b).

5.3.2.2 Specimen Strength and Interstory Drift

The specimen strength can be represented by a plot of the column shear force versus interstory drift (figure 5-14(a,b)). Column shear force was taken such that the zero value corresponded

to the shear force due to the gravity effects. From these hysteresis plots, column shear capacity envelopes were generated by connecting the peak points of each hysteresis loop. Figure 5-15 shows these envelopes for both the non-retrofitted and the retrofitted specimens. Since the concrete strength of the joint governed the overall capacity, plots starting from figures 5-15 to 5-17 were normalized by $\sqrt{f'_c}$ (f'_c is the measured compressive strength of the concrete in the joint-panel and the beams). The f'_c values were 4220 and 3070 psi for specimens E-07 and RE-1 respectively.



FIGURE 5-13 Photo Taken After the Test (exterior)

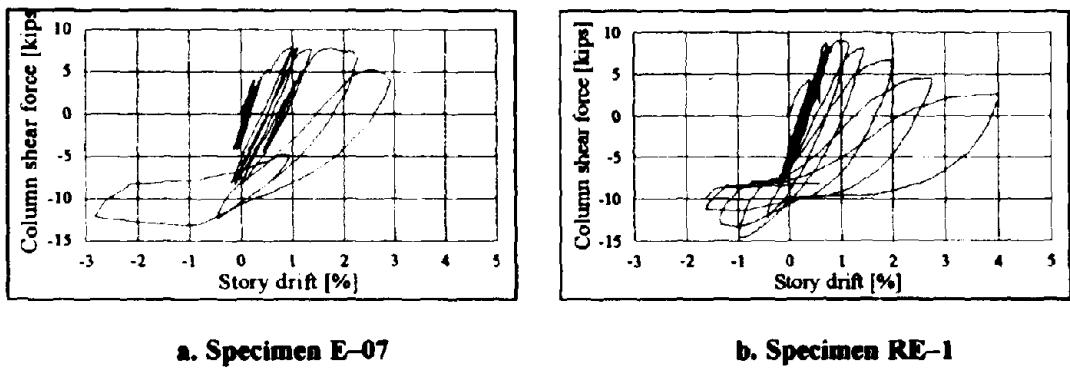


FIGURE 5-14 Column Shear-Interstory Drift (exterior)

Figure 5-15 shows an increase in strength due to the retrofit up to about 1.75% interstory drift. The peak strength was increased by about 33%. The retrofitted specimen showed a higher rate of strength loss after the peak strength.

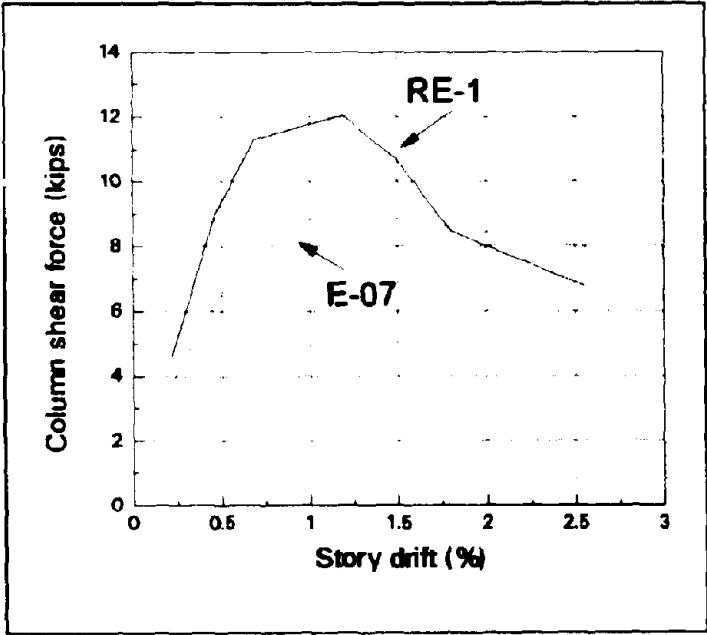


FIGURE 5-15 Column Shear Force Versus Interstory Drift Envelopes (exterior)

5.3.2.3 Specimen Stiffness

Stiffness degradation is illustrated by a plot of the specimen stiffness versus the average of the absolute maximum values of the positive and negative interstory drifts, as shown in figure 5-16. The specimen stiffness corresponds to the peak-to-peak slope of each cycle in the column shear versus interstory drift.

The retrofit scheme resulted in a slight increase in the initial stiffness (about 12%). Stiffness degradation rates for both specimens were similar up to about an interstory drift value of 1.3%. At that point pullout of the embedded positive beam reinforcement occurred only in the retrofitted specimen. This explains the slightly higher stiffness loss in the retrofitted specimen.

Although stiffness degradation in an exterior joint might sound alarming, the overall stiffness degradation of an actual LRC building could be kept to a minimum if there were a sufficient number of interior joint regions in which only a small loss of stiffness takes place.

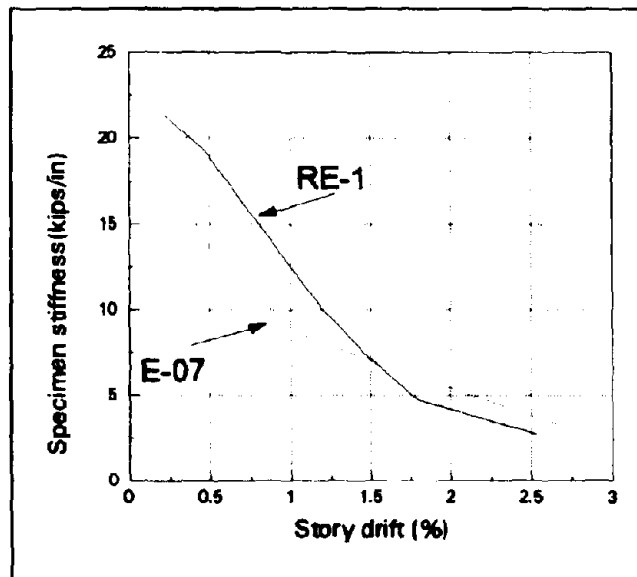


FIGURE 5-16 Stiffness vs. Maximum Interstory Drift (exterior)

5.3.2.4 Energy Dissipation

Energy dissipation is represented by a plot of the cumulative dissipated energy versus the average of the absolute peak values of the positive and negative interstory drifts, as shown in figure 5-17. The cumulative dissipated energy was computed by summing the area enclosed within the column shear versus average interstory drift. This is an approximation because of frictional losses induced during the test.

Figure 5-17 shows that energy dissipation was about the same for both non-retrofitted and retrofitted specimens up to an average drift value of 1.3%. After that point, the retrofit scheme resulted in a significant (about 230%) increase in the rate of energy dissipation. This is due to the inelastic bending of the 1/2 inch thick back plate, as indicated on the permanent flexural deformations observed after the test. It is interesting to note that energy dissipation started to increase at about the same drift (1.3%) that stiffness started to decrease (comparing figures 5-16 and 5-17). Pullout of the embedded positive beam reinforcement resulted in higher bending rotations in the 1/2 inch thick back plate.

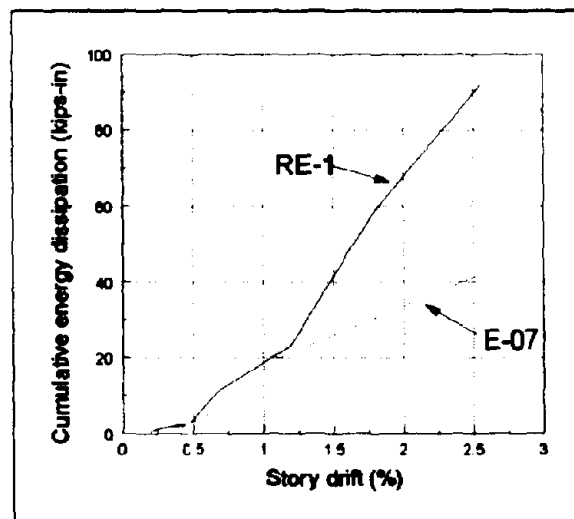


FIGURE 5-17 Cumulative Energy Dissipation vs. Interstory Drift (exterior)

5.3.3 Summary

A practical, inexpensive retrofit scheme was developed and tested on an exterior joint component. The retrofitting produced major changes in the damage mechanisms. These changes included the formation of a flexural hinge in the joint panel zone close to the beam, the protection of the back concrete cover, and the prevention of cracks from extending into the top column splice region. An increase in the peak strength was observed followed by a higher deterioration rate compared to the bare specimen. The initial stiffness was slightly increased, while the degradation rate was about the same up to the point where the pullout of the embedded bottom beam reinforcement occurred. A significant increase in the energy dissipation capacity was observed.

SECTION 6

SUMMARY, CONCLUSIONS, AND SUGGESTIONS FOR FUTURE RESEARCH

6.1 Summary and Conclusions

This report summarizes the current experimental work at Cornell University concerning the repair and retrofit of lightly reinforced concrete structures. Lightly reinforced concrete framing, designed primarily for the effects of gravity loads with little or no attention given to lateral load effects, is characterized by the following details: no more than about 2% longitudinal column reinforcement with lap splices located immediately above floor levels in the zone of maximum seismic moment; widely spaced column ties; little or no transverse reinforcement within the joint region; and discontinuous positive moment beam reinforcement with a 6 inch embedment length into the column.

A total of 34 interior and exterior beam-column joints were tested to identify the different damage mechanisms and study the effect of critical details. The most important findings are summarized in Section 3. One of the tested interior specimens was repaired and retested, using the vacuum resin injection technique as described in Section 4. In addition, two virgin specimens (one interior and one exterior) were retrofitted with externally attached steel plates as discussed in Section 5.

6.1.1 Repaired Specimen

Resin impregnation by a special vacuum technology was used to repair a heavily cracked specimen in order to improve the structural integrity and the cyclic load capacity. Vacuum impregnation was chosen versus the conventional pressure injection technique because it is hoped that it would provide better bonding capacity.

The repaired specimen reached a value of about 72% of the peak column shear capacity of the original specimen. The failure of the repaired specimen to maintain load capacity beyond 5 or 6 cycles was attributed to the pullout of the embedded bottom rebars of the beams. Heavy concrete damage was visible around the embedment zone with the main diagonal cracks going through this region

Other performance characteristics were favorable. Since only portions of the cracked zones were repaired, the initial stiffness of REP I-11 was about 25% less than that of the virgin specimen. The repair scheme resulted in a similar stiffness degradation rate with convergence at high deformations. Energy dissipation was almost identical for the repaired and the virgin specimens. The slightly higher cumulative energy values for I-11 are attributed to the fact that only cracks close to the joint-panel zone were filled with resin and few new cracks developed outside this region during the retest. Beyond 2% drift, substantial cracking and loss of stiffness occurred in both cases. This caused an increase in the energy dissipation rate. Because of the limited experimental evidence, it is difficult to come up with firm conclusions. Possible directions of further research are outlined in Section 4.3.

6.1.2 Retrofitted Specimen

Two common joint configurations were considered for retrofit – interior and exterior joints with discontinuous bottom beam reinforcement. The capacity of the bare interior specimen was controlled by pullout of the discontinuous bottom beam reinforcement, while the failure of the exterior specimen occurred by a combination of (a) excessive diagonal shear cracking followed by splice failure in the top column; (b) spalling of the concrete cover due to the prying action of the bent-down negative beam reinforcement; and (c) to a smaller extent pullout of the embedded bottom beam reinforcement.

Based on the previously mentioned experimental behavior of the bare specimens, preliminary analytical predictions, and input from consulting practicing engineers, retrofit schemes were designed for each joint configuration. These schemes, aimed at retrofitting structures in zones of moderate seismicity, consisted of attaching external steel plates, as shown in figures 5-1 and 5-10. This type of retrofit was particularly appealing for several reasons:

1. It provides freedom in the custom-tailoring of the retrofit, so different damage mechanisms and specimen geometries can be addressed with the same technology.
2. Being local retrofit, it does not interfere with the original building space use.
3. It is relatively unobtrusive.
4. It does not increase significantly the initial stiffness of the frame, thus protecting the structure from moving up on the response spectrum curve.
5. It should provide fast and inexpensive installation, with minimum disturbance of the normal building functions.

The local damage mechanism was altered markedly in both cases:

- (i) For the interior specimen, pullout of the positive beam reinforcement was successfully prevented. Damage was transferred from the embedment zone to other parts of the joint panel, and to a smaller extent to the top of the beam and to the upper construction joint. The retrofit slightly increased the column shear strength and reduced the deterioration rate. The stiffness characteristics were about the same, and the energy dissipation did not change. Tests done on a bare interior joint with continuous reinforcement and similar parameters to the retrofitted specimen showed closely matching strength results and deterioration mode. Because of the low column-to-beam flexural strength and the

nonductile detailing of the joint-panel this type of retrofit may result in undesirable soft-story mechanism. Therefore, the careful analysis of the entire structure is suggested.

- (ii) For the exterior specimen, significant changes in the behavior were observed. These included the formation of a flexural hinge in the joint panel zone close to the beam, the protection of the back concrete cover, and the prevention of cracks from extending into the top column splice region. The retrofit increased the peak strength and to a smaller extent the initial stiffness. The strength deterioration rate was higher after the peak strength. The stiffness loss was about the same up to the point where the pullout of the embedded bottom beam reinforcement occurred. A notable increase in the energy dissipation capacity was achieved in the final stages of the test.

In the analysis of buildings, displacements of columns at the same floor are frequently assumed to be identical. This provides a basis of comparison between interior and exterior retrofitted joints. As shown in figures 5-7 and 5-15, both specimens showed an increase of strength up to about 1.3% interstory drift. Beyond this point, the exterior joint exhibited a rapid decrease in strength, while the interior joint maintained its shear capacity.

Although the simple retrofit schemes implemented in this study proved to be viable means of altering certain local damage mechanisms special attention is necessary to avoid unfavorable mechanisms. In interior joints the proposed upgrade may work well at the lower stories of taller buildings, but at the upper levels weak column mechanisms may develop.

6.2 Recommendations for Future Research

This report summarizes a preliminary investigation on the retrofit of LRC structures. Clearly more tests and analyses are needed to make more definitive conclusions. The following topics still need to be addressed to gain a better understanding of repairing and retrofitting this class of buildings:

1. Additional tests with different repair and retrofit schemes are needed to devise strategies that result in better overall building performance.
2. Analytical tools to predict the response of the repaired and retrofitted joints need to be enhanced and calibrated based on experimental results.
3. A series of analytical predictions of typical repaired and retrofitted LRC structures has to be performed.
4. Evaluation criteria for acceptable building performance should be developed.

SECTION 7

PUBLICATIONS CITED

- ACI Committee 315, *Manual of Standard Practice for Detailing Reinforced Concrete Structures*, American Concrete Institute, Detroit, MI, 1948, 1951, 1957, 1965, 1974.
- ACI Committee 318, *Building Code Requirements for Reinforced Concrete*, American Concrete Institute, Detroit, MI, 1951, 1956, 1963, 1971, 1983, 1989.
- ACI-ASCE Committee 352, *Recommendations for Design of Beam-Column Joints in Monolithic Reinforced Concrete Structures, (ACI 352R-91)*, American Concrete Institute, Detroit, MI, 1991.
- Bertero, V. V., and Popov, E. P., "Seismic Behavior of Ductile Moment-Resisting Reinforced Concrete Frames," *Reinforced Concrete Structures in Seismic Zones*, American Concrete Institute SP-53, Detroit, 1977, pp. 247-291.
- Bracci, J. M., Reinhorn, A. M., Mander, J. B., *Evaluation of Seismic Retrofit of Reinforced Concrete Frame Structures, Part I: Experimental Performance and Analytical Study of Retrofitted Structural Model*, Technical Report, NCEER-92-0031 National Center for Earthquake Engineering Research, State University of New York at Buffalo, 1992.
- Beres, A., Pessiki, S. P., Gergely, P., and White R.N., "Behavior of Existing Reinforced Concrete Frames Designed Primarily for Gravity Loads," *Proceedings of the International Meeting on Earthquake Protection of Buildings*, Ancona, Italy, 1991, Section B, pp. 75-86.
- Choudhuri, L. E., Mander, J. B., and Reinhorn, A. M., *Evaluation of Seismic Retrofit of R/C Frame Structures, Part II: Experimental Performance of Retrofitted Subassemblages*, Technical Report, NCEER-92-0030, National Center for Earthquake Engineering Research, State University of New York at Buffalo, 1992.
- Corazao, M., Durrani, A. J., *Repair and Strengthening of Beam-To-Column Connections Subjected to Earthquake Loading*, Technical Report, NCEER-89-0013, National Center for Earthquake Engineering Research, State University of New York at Buffalo, 1989.

APPENDIX

Technological Comments About Adhesive Anchor Installation

There are different ways to fix anchors to the concrete. The system used has two main components: an adhesive capsule and a stud rod. The installation is done by driving the stud rod through the capsule (placed beforehand in the hole) with a rotary percussion hammer-drill. As the stud breaks the capsule, the crushed glass, the aggregate and the adhesive form a permanent bond between the rod and the concrete. The rod is embedded evenly along the entire length eliminating single point stress concentration, therefore providing excellent bearing for vibratory loading. Although in case of seismic loading only a few dozen cycles are expected, this method is believed to serve more reliably than mechanical fixing of the studs, for example, undercut anchors. The installation steps are the following:

1. The steel plates with predrilled holes are covered with a layer of mortar and fixed in position at the underside of the beam with clamps. This step could be postponed, however attaching the plates after the studs are fixed in place might require precision that is unsuitable at the field.
2. Drill holes using the steel plates as a template to the required length as specified by the manufacturer. A hole diameter only 1/16" larger than the nominal bolt diameter was found satisfactory.
3. Remove dust from the hole with pressurized air or water-jet.
4. Insert the capsule into the hole with the rounded end facing the back of the hole. The capsule is a double glass-tube separating the epoxy resin and the hardener. It also contains some fine aggregate.

5. **Attach a custom-made setting tool to the chuck of the rotary percussion hammer-drill (to facilitate the removal of the handhold drill afterwards).**
6. **Fix a stud-rod with a plastic collar and a nut onto the setting tool. The plastic collar protects the drill and its operator from the potential leakage and spraying of the adhesive.**
7. **Drive the stud-rod to the bottom of the hole breaking through the capsule.**
8. **After about one minute the adhesive sets. First the drill and then the setting tool can be removed.**
9. **After a short curing period (10 min. to 5 hour depending on the temperature) remove the plastic collar and load the rods. High torque is not required to utilize fully the strength of the stud-rods.**

**NATIONAL CENTER FOR EARTHQUAKE ENGINEERING RESEARCH
LIST OF TECHNICAL REPORTS**

The National Center for Earthquake Engineering Research (NCEER) publishes technical reports on a variety of subjects related to earthquake engineering written by authors funded through NCEER. These reports are available from both NCEER's Publications Department and the National Technical Information Service (NTIS). Requests for reports should be directed to the Publications Department, National Center for Earthquake Engineering Research, State University of New York at Buffalo, Red Jacket Quadrangle, Buffalo, New York 14261. Reports can also be requested through NTIS, 5285 Port Royal Road, Springfield, Virginia 22161. NTIS accession numbers are shown in parenthesis, if available.

- NCEER-87-0001 "First-Year Program in Research, Education and Technology Transfer," 3/5/87, (PB88-134275/AS).
- NCEER-87-0002 "Experimental Evaluation of Instantaneous Optimal Algorithms for Structural Control," by R.C. Lin, T.T. Soong and A.M. Reinhorn, 4/20/87, (PB88-134341/AS).
- NCEER-87-0003 "Experimentation Using the Earthquake Simulation Facilities at University at Buffalo," by A.M. Reinhorn and R.L. Ketter, to be published.
- NCEER-87-0004 "The System Characteristics and Performance of a Shaking Table," by J.S. Hwang, K.C. Chang and G.C. Lee, 6/1/87, (PB88-134259/AS). This report is available only through NTIS (see address given above).
- NCEER-87-0005 "A Finite Element Formulation for Nonlinear Viscoplastic Material Using a Q Model," by O. Gyebi and G. Dasgupta, 11/2/87, (PB88-213764/AS).
- NCEER-87-0006 "Symbolic Manipulation Program (SMP) - Algebraic Codes for Two and Three Dimensional Finite Element Formulations," by X. Lee and G. Dasgupta, 11/9/87, (PB88-219522/AS).
- NCEER-87-0007 "Instantaneous Optimal Control Laws for Tall Buildings Under Seismic Excitations," by J.N. Yang, A. Akbarpour and P. Ghaemmaghami, 6/10/87, (PB88-134333/AS).
- NCEER-87-0008 "IDARC: Inelastic Damage Analysis of Reinforced Concrete Frame - Shear-Wall Structures," by Y.J. Park, A.M. Reinhorn and S.K. Kunath, 7/20/87, (PB88-134325/AS).
- NCEER-87-0009 "Liquefaction Potential for New York State: A Preliminary Report on Sites in Manhattan and Buffalo," by M. Budhu, V. Vijayakumar, R.F. Giese and L. Baumgras, 8/31/87, (PB88-163704/AS). This report is available only through NTIS (see address given above).
- NCEER-87-0010 "Vertical and Torsional Vibration of Foundations in Inhomogeneous Media," by A.S. Veletsos and K.W. Dotson, 6/1/87, (PB88-134291/AS).
- NCEER-87-0011 "Seismic Probabilistic Risk Assessment and Seismic Margins Studies for Nuclear Power Plants," by Howard H.M. Hwang, 6/15/87, (PB88-134267/AS).
- NCEER-87-0012 "Parametric Studies of Frequency Response of Secondary Systems Under Ground-Acceleration Excitations," by Y. Yong and Y.K. Lin, 6/10/87, (PB88-134309/AS).
- NCEER-87-0013 "Frequency Response of Secondary Systems Under Seismic Excitation," by J.A. HoLung, J. Cai and Y.K. Lin, 7/31/87, (PB88-134317/AS).
- NCEER-87-0014 "Modelling Earthquake Ground Motions in Seismically Active Regions Using Parametric Time Series Methods," by G.W. Ellis and A.S. Cakmak, 8/25/87, (PB88-134283/AS).
- NCEER-87-0015 "Detection and Assessment of Seismic Structural Damage," by E. DiPasquale and A.S. Cakmak, 8/25/87, (PB88-163712/AS).

- NCEER-87-0016 "Pipeline Experiment at Parkfield, California," by J. Isenberg and E. Richardson, 9/15/87, (PB88-163720/AS). This report is available only through NTIS (see address given above).
- NCEER-87-0017 "Digital Simulation of Seismic Ground Motion," by M. Shinozuka, G. Deodatis and T. Harada, 8/31/87, (PB88-155197/AS). This report is available only through NTIS (see address given above).
- NCEER-87-0018 "Practical Considerations for Structural Control: System Uncertainty, System Time Delay and Truncation of Small Control Forces," J.N. Yang and A. Akbarpour, 8/10/87, (PB88-163738/AS).
- NCEER-87-0019 "Modal Analysis of Nonclassically Damped Structural Systems Using Canonical Transformation," by J.N. Yang, S. Sarkani and F.X. Long, 9/27/87, (PB88-187851/AS).
- NCEER-87-0020 "A Nonstationary Solution in Random Vibration Theory," by J.R. Red-Horse and P.D. Spanos, 11/3/87, (PB88-163746/AS).
- NCEER-87-0021 "Horizontal Impedances for Radially Inhomogeneous Viscoelastic Soil Layers," by A.S. Veletsos and K.W. Dotson, 10/15/87, (PB88-150859/AS).
- NCEER-87-0022 "Seismic Damage Assessment of Reinforced Concrete Members," by Y.S. Chung, C. Meyer and M. Shinozuka, 10/9/87, (PB88-150867/AS). This report is available only through NTIS (see address given above).
- NCEER-87-0023 "Active Structural Control in Civil Engineering," by T.T. Soong, 11/11/87, (PB88-187778/AS).
- NCEER-87-0024 "Vertical and Torsional Impedances for Radially Inhomogeneous Viscoelastic Soil Layers," by K.W. Dotson and A.S. Veletsos, 12/87, (PB88-187786/AS).
- NCEER-87-0025 "Proceedings from the Symposium on Seismic Hazards, Ground Motions, Soil-Liquefaction and Engineering Practice in Eastern North America," October 20-22, 1987, edited by K.H. Jacob, 12/87, (PB88-188115/AS).
- NCEER-87-0026 "Report on the Whittier-Narrows, California, Earthquake of October 1, 1987," by J. Pantelic and A. Reinhorn, 11/87, (PB88-187752/AS). This report is available only through NTIS (see address given above).
- NCEER-87-0027 "Design of a Modular Program for Transient Nonlinear Analysis of Large 3-D Building Structures," by S. Srivastav and J.F. Abel, 12/30/87, (PB88-187950/AS).
- NCEER-87-0028 "Second-Year Program in Research, Education and Technology Transfer," 3/8/88, (PB88-219480/AS).
- NCEER-88-0001 "Workshop on Seismic Computer Analysis and Design of Buildings With Interactive Graphics," by W. McGuire, J.F. Abel and C.H. Conley, 1/18/88, (PB88-187760/AS).
- NCEER-88-0002 "Optimal Control of Nonlinear Flexible Structures," by J.N. Yang, F.X. Long and D. Wong, 1/22/88, (PB88-213772/AS).
- NCEER-88-0003 "Substructuring Techniques in the Time Domain for Primary-Secondary Structural Systems," by G.D. Manolis and G. Juhn, 2/10/88, (PB88-213780/AS).
- NCEER-88-0004 "Iterative Seismic Analysis of Primary-Secondary Systems," by A. Singhal, L.D. Lutes and P.D. Spanos, 2/23/88, (PB88-213798/AS).
- NCEER-88-0005 "Stochastic Finite Element Expansion for Random Media," by P.D. Spanos and R. Ghanem, 3/14/88, (PB88-213806/AS).

- NCEER-88-0006 "Combining Structural Optimization and Structural Control," by F.Y. Cheng and C.P. Pantelides, 1/10/88, (PB88-213814/AS).
- NCEER-88-0007 "Seismic Performance Assessment of Code-Designed Structures," by H.H.-M. Hwang, J.-W. Jaw and H.-J. Shau, 3/20/88, (PB88-219423/AS).
- NCEER-88-0008 "Reliability Analysis of Code-Designed Structures Under Natural Hazards," by H.H.-M. Hwang, H. Ushiba and M. Shinozuka, 2/29/88, (PB88-229471/AS).
- NCEER-88-0009 "Seismic Fragility Analysis of Shear Wall Structures," by J.-W. Jaw and H.H.-M. Hwang, 4/30/88, (PB89-102867/AS).
- NCEER-88-0010 "Base Isolation of a Multi-Story Building Under a Harmonic Ground Motion - A Comparison of Performances of Various Systems," by F.-G. Fan, G. Ahmadi and I.G. Tadjbakhsh, 5/18/88, (PB89-122238/AS).
- NCEER-88-0011 "Seismic Floor Response Spectra for a Combined System by Green's Functions," by F.M. Lavelle, L.A. Bergman and P.D. Spanos, 5/1/88, (PB89-102875/AS).
- NCEER-88-0012 "A New Solution Technique for Randomly Excited Hysteretic Structures," by G.Q. Cai and Y.K. Lin, 5/16/88, (PB89-102883/AS).
- NCEER-88-0013 "A Study of Radiation Damping and Soil-Structure Interaction Effects in the Centrifuge," by K. Weissman, supervised by J.H. Prevost, 5/24/88, (PB89-144703/AS).
- NCEER-88-0014 "Parameter Identification and Implementation of a Kinematic Plasticity Model for Frictional Soils," by J.H. Prevost and D.V. Griffiths, to be published.
- NCEER-88-0015 "Two- and Three- Dimensional Dynamic Finite Element Analyses of the Long Valley Dam," by D.V. Griffiths and J.H. Prevost, 6/17/88, (PB89-144711/AS).
- NCEER-88-0016 "Damage Assessment of Reinforced Concrete Structures in Eastern United States," by A.M. Reinhorn, M.J. Seidel, S.K. Kunnath and Y.J. Park, 6/15/88, (PB89-122220/AS).
- NCEER-88-0017 "Dynamic Compliance of Vertically Loaded Strip Foundations in Multilayered Viscoelastic Soils," by S. Ahmad and A.S.M. Israil, 6/17/88, (PB89-102891/AS).
- NCEER-88-0018 "An Experimental Study of Seismic Structural Response With Added Viscoelastic Dampers," by R.C. Lin, Z. Liang, T.T. Soong and R.H. Zhang, 6/30/88, (PB89-122212/AS). This report is available only through NTIS (see address given above).
- NCEER-88-0019 "Experimental Investigation of Primary - Secondary System Interaction," by G.D. Manolis, G. Juhn and A.M. Reinhorn, 5/27/88, (PB89-122204/AS).
- NCEER-88-0020 "A Response Spectrum Approach For Analysis of Nonclassically Damped Structures," by J.N. Yang, S. Sarkani and F.X. Long, 4/22/88, (PB89-102909/AS).
- NCEER-88-0021 "Seismic Interaction of Structures and Soils: Stochastic Approach," by A.S. Veletsos and A.M. Prasad, 7/21/88, (PB89-122196/AS).
- NCEER-88-0022 "Identification of the Serviceability Limit State and Detection of Seismic Structural Damage," by E. DiPasquale and A.S. Cakmak, 6/15/88, (PB89-122188/AS). This report is available only through NTIS (see address given above).
- NCEER-88-0023 "Multi-Hazard Risk Analysis: Case of a Simple Offshore Structure," by B.K. Bhartia and E.H. Vanmarcke, 7/21/88, (PB89-145213/AS).

- NCEER-88-0024 "Automated Seismic Design of Reinforced Concrete Buildings," by Y.S. Chung, C. Meyer and M. Shinozuka, 7/5/88, (PB89-122170/AS). This report is available only through NTIS (see address given above).
- NCEER-88-0025 "Experimental Study of Active Control of MDOF Structures Under Seismic Excitations," by L.L. Chung, R.C. Lin, T.T. Soong and A.M. Reinhorn, 7/10/88, (PB89-122600/AS).
- NCEER-88-0026 "Earthquake Simulation Tests of a Low-Rise Metal Structure," by J.S. Hwang, K.C. Chang, G.C. Lee and R.L. Ketter, 8/1/88, (PB89-102917/AS).
- NCEER-88-0027 "Systems Study of Urban Response and Reconstruction Due to Catastrophic Earthquakes," by F. Kozin and H.K. Zhou, 9/22/88, (PB90-162348/AS).
- NCEER-88-0028 "Seismic Fragility Analysis of Plane Frame Structures," by H.H.M. Hwang and Y.K. Low, 7/31/88, (PB89-131445/AS).
- NCEER-88-0029 "Response Analysis of Stochastic Structures," by A. Kardara, C. Bucher and M. Shinozuka, 9/22/88, (PB89-174429/AS).
- NCEER-88-0030 "Nonnormal Accelerations Due to Yielding in a Primary Structure," by D.C.K. Chen and L.D. Lutes, 9/19/88, (PB89-131437/AS).
- NCEER-88-0031 "Design Approaches for Soil-Structure Interaction," by A.S. Veletsos, A.M. Prasad and Y. Tang, 12/30/88, (PB89-174437/AS). This report is available only through NTIS (see address given above).
- NCEER-88-0032 "A Re-evaluation of Design Spectra for Seismic Damage Control," by C.J. Turkstra and A.G. Tallin, 11/7/88, (PB89-145221/AS).
- NCEER-88-0033 "The Behavior and Design of Noncontact Lap Splices Subjected to Repeated Inelastic Tensile Loading," by V.E. Sagan, P. Gergely and R.N. White, 12/8/88, (PB89-163737/AS).
- NCEER-88-0034 "Seismic Response of Pile Foundations," by S.M. Marnoon, P.K. Banerjee and S. Ahmad, 11/1/88, (PB89-145239/AS).
- NCEER-88-0035 "Modeling of R/C Building Structures With Flexible Floor Diaphragms (IDARC2)," by A.M. Reinhorn, S.K. Kunnath and N. Panahshahi, 9/7/88, (PB89-207153/AS).
- NCEER-88-0036 "Solution of the Dam-Reservoir Interaction Problem Using a Combination of FEM, BEM with Particular Integrals, Modal Analysis, and Substructuring," by C-S. Tsai, G.C. Lee and R.L. Ketter, 12/31/88, (PB89-207146/AS).
- NCEER-88-0037 "Optimal Placement of Actuators for Structural Control," by F.Y. Cheng and C.P. Pantelides, 8/15/88, (PB89-162846/AS).
- NCEER-88-0038 "Teflon Bearings in Aseismic Base Isolation: Experimental Studies and Mathematical Modeling," by A. Mokha, M.C. Constantinou and A.M. Reinhorn, 12/5/88, (PB89-218457/AS). This report is available only through NTIS (see address given above).
- NCEER-88-0039 "Seismic Behavior of Flat Slab High-Rise Buildings in the New York City Area," by P. Weidlinger and M. Etouney, 10/15/88, (PB90-145681/AS).
- NCEER-88-0040 "Evaluation of the Earthquake Resistance of Existing Buildings in New York City," by P. Weidlinger and M. Etouney, 10/15/88, to be published.
- NCEER-88-0041 "Small-Scale Modeling Techniques for Reinforced Concrete Structures Subjected to Seismic Loads," by W. Kim, A. El-Attar and R.N. White, 11/22/88, (PB89-189625/AS).

- NCEER-88-0042 "Modeling Strong Ground Motion from Multiple Event Earthquakes," by G.W. Ellis and A.S. Cakmak, 10/15/88, (PB89-174445/AS).
- NCEER-88-0043 "Nonstationary Models of Seismic Ground Acceleration," by M. Grigoriu, S.E. Ruiz and E. Rosenblueth, 7/15/88, (PB89-189617/AS).
- NCEER-88-0044 "SARCF User's Guide: Seismic Analysis of Reinforced Concrete Frames," by Y.S. Chung, C. Meyer and M. Shinozuka, 11/9/88, (PB89-174452/AS).
- NCEER-88-0045 "First Expert Panel Meeting on Disaster Research and Planning," edited by J. Pantelic and J. Stoyke, 9/15/88, (PB89-174460/AS).
- NCEER-88-0046 "Preliminary Studies of the Effect of Degrading Infill Walls on the Nonlinear Seismic Response of Steel Frames," by C.Z. Chrysostomou, P. Gergely and J.F. Abel, 12/19/88, (PB89-208383/AS).
- NCEER-88-0047 "Reinforced Concrete Frame Component Testing Facility - Design, Construction, Instrumentation and Operation," by S.P. Pessiki, C. Conley, T. Bond, P. Gergely and R.N. White, 12/16/88, (PB89-174478/AS).
- NCEER-89-0001 "Effects of Protective Cushion and Soil Compliancy on the Response of Equipment Within a Seismically Excited Building," by J.A. HoLung, 2/16/89, (PB89-207179/AS).
- NCEER-89-0002 "Statistical Evaluation of Response Modification Factors for Reinforced Concrete Structures," by H.H.M. Hwang and J.W. Jaw, 2/17/89, (PB89-207187/AS).
- NCEER-89-0003 "Hysteretic Columns Under Random Excitation," by G-Q. Cai and Y.K. Lin, 1/9/89, (PB89-196513/AS).
- NCEER-89-0004 "Experimental Study of 'Elephant Foot Bulge' Instability of Thin-Walled Metal Tanks," by Z-H. Jia and R.L. Ketter, 2/22/89, (PB89-207195/AS).
- NCEER-89-0005 "Experiment on Performance of Buried Pipelines Across San Andreas Fault," by J. Isenberg, E. Richardson and T.D. O'Rourke, 3/10/89, (PB89-218440/AS).
- NCEER-89-0006 "A Knowledge-Based Approach to Structural Design of Earthquake-Resistant Buildings," by M. Subramani, P. Gergely, C.H. Conley, J.F. Abel and A.H. Zaghw, 1/15/89, (PB89-218465/AS).
- NCEER-89-0007 "Liquefaction Hazards and Their Effects on Buried Pipelines," by T.D. O'Rourke and P.A. Lane, 2/1/89, (PB89-218481).
- NCEER-89-0008 "Fundamentals of System Identification in Structural Dynamics," by H. Imai, C-B. Yun, O. Maruyama and M. Shinozuka, 1/26/89, (PB89-207211/AS).
- NCEER-89-0009 "Effects of the 1985 Michoacan Earthquake on Water Systems and Other Buried Lifelines in Mexico," by A.G. Ayala and M.J. O'Rourke, 3/8/89, (PB89-207229/AS).
- NCEER-89-R010 "NCEER Bibliography of Earthquake Education Materials," by K.E.K. Ross, Second Revision, 9/1/89, (PB90-125352/AS).
- NCEER-89-0011 "Inelastic Three-Dimensional Response Analysis of Reinforced Concrete Building Structures (IDARC-3D), Part I - Modeling," by S.K. Kunnath and A.M. Reinhorn, 4/17/89, (PB90-114612/AS).
- NCEER-89-0012 "Recommended Modifications to ATC-14," by C.D. Poland and J.O. Malley, 4/12/89, (PB90-108648/AS).
- NCEER-89-0013 "Repair and Strengthening of Beam-to-Column Connections Subjected to Earthquake Loading," by M. Corazao and A.J. Durrani, 2/28/89, (PB90-109885/AS).

- NCEER-89-0014 "Program EXKAL2 for Identification of Structural Dynamic Systems," by O. Maruyama, C-B. Yun, M. Hoshiya and M. Shinozuka, 5/19/89, (PB90-109877/AS).
- NCEER-89-0015 "Response of Frames With Bolted Semi-Rigid Connections, Part I - Experimental Study and Analytical Predictions," by P.J. DiCorso, A.M. Reinhorn, J.R. Dickerson, J.B. Radzimirski and W.L. Harper, 6/1/89, to be published.
- NCEER-89-0016 "ARMA Monte Carlo Simulation in Probabilistic Structural Analysis," by P.D. Spanos and M.P. Mignolet, 7/10/89, (PB90-109893/AS).
- NCEER-89-P017 "Preliminary Proceedings from the Conference on Disaster Preparedness - The Place of Earthquake Education in Our Schools," Edited by K.E.K. Ross, 6/23/89.
- NCEER-89-0017 "Proceedings from the Conference on Disaster Preparedness - The Place of Earthquake Education in Our Schools," Edited by K.E.K. Ross, 12/31/89, (PB90-207895). This report is available only through NTIS (see address given above).
- NCEER-89-0018 "Multidimensional Models of Hysteretic Material Behavior for Vibration Analysis of Shape Memory Energy Absorbing Devices, by E.J. Graesser and F.A. Cozzarelli, 6/7/89, (PB90-164146/AS).
- NCEER-89-0019 "Nonlinear Dynamic Analysis of Three-Dimensional Base Isolated Structures (3D-BASIS)," by S. Nagarajaiah, A.M. Reinhorn and M.C. Constantinou, 8/3/89, (PB90-161936/AS). This report is available only through NTIS (see address given above).
- NCEER-89-0020 "Structural Control Considering Time-Rate of Control Forces and Control Rate Constraints," by F.Y. Cheng and C.P. Panteides, 8/3/89, (PB90-120445/AS).
- NCEER-89-0021 "Subsurface Conditions of Memphis and Shelby County," by K.W. Ng, T-S. Chang and H-H.M. Hwang, 7/26/89, (PB90-120437/AS).
- NCEER-89-0022 "Seismic Wave Propagation Effects on Straight Jointed Buried Pipelines," by K. Elhadi and M.J. O'Rourke, 8/24/89, (PB90-162322/AS).
- NCEER-89-0023 "Workshop on Serviceability Analysis of Water Delivery Systems," edited by M. Grigoriu, 3/6/89, (PB90-127424/AS).
- NCEER-89-0024 "Shaking Table Study of a 1/5 Scale Steel Frame Composed of Tapered Members," by K.C. Chang, J.S. Hwang and G.C. Lee, 9/18/89, (PB90-160169/AS).
- NCEER-89-0025 "DYNA1D: A Computer Program for Nonlinear Seismic Site Response Analysis - Technical Documentation," by Jean H. Prevost, 9/14/89, (PB90-161944/AS). This report is available only through NTIS (see address given above).
- NCEER-89-0026 "1:4 Scale Model Studies of Active Tendon Systems and Active Mass Dampers for Aseismic Protection," by A.M. Reinhorn, T.T. Soong, R.C. Lin, Y.P. Yang, Y. Fukao, H. Abe and M. Nakai, 9/15/89, (PB90-173246/AS).
- NCEER-89-0027 "Scattering of Waves by Inclusions in a Nonhomogeneous Elastic Half Space Solved by Boundary Element Methods," by P.K. Hadley, A. Askar and A.S. Cakma', 6/15/89, (PB90-145699/AS).
- NCEER-89-0028 "Statistical Evaluation of Deflection Amplification Factors for Reinforced Concrete Structures," by H.H.M. Hwang, J-W. Jaw and A.L. Ch'ng, 8/31/89, (PB90-164633/AS).
- NCEER-89-0029 "Bedrock Accelerations in Memphis Area Due to Large New Madrid Earthquakes," by H.H.M. Hwang, C.H.S. Chen and G. Yu, 11/7/89, (PB90-162330/AS).

- NCEER-89-0030 "Seismic Behavior and Response Sensitivity of Secondary Structural Systems," by Y.Q. Chen and T.T. Soong, 10/23/89, (PB90-164658/AS).
- NCEER-89-0031 "Random Vibration and Reliability Analysis of Primary-Secondary Structural Systems," by Y. Ibrahim, M. Grigoriu and T.T. Soong, 11/10/89, (PB90-161951/AS).
- NCEER-89-0032 "Proceedings from the Second U.S. - Japan Workshop on Liquefaction, Large Ground Deformation and Their Effects on Lifelines, September 26-29, 1989," Edited by T.D. O'Rourke and M. Hamada, 12/1/89, (PB90-209388/AS).
- NCEER-89-0033 "Deterministic Model for Seismic Damage Evaluation of Reinforced Concrete Structures," by J.M. Bracci, A.M. Reinhorn, J.B. Mander and S.K. Kunnath, 9/27/89.
- NCEER-89-0034 "On the Relation Between Local and Global Damage Indices," by E. DiPasquale and A.S. Cakmak, 8/15/89, (PB90-173865).
- NCEER-89-0035 "Cyclic Undrained Behavior of Nonplastic and Low Plasticity Silts," by A.J. Walker and H.E. Stewart, 7/26/89, (PB90-183518/AS).
- NCEER-89-0036 "Liquefaction Potential of Surficial Deposits in the City of Buffalo, New York," by M. Budhu, R. Giese and L. Baumgrass, 1/17/89, (PB90-208455/AS).
- NCEER-89-0037 "A Deterministic Assessment of Effects of Ground Motion Incoherence," by A.S. Veletsos and Y. Tang, 7/15/89, (PB90-164294/AS).
- NCEER-89-0038 "Workshop on Ground Motion Parameters for Seismic Hazard Mapping," July 17-18, 1989, edited by R.V. Whitman, 12/1/89, (PB90-173923/AS).
- NCEER-89-0039 "Seismic Effects on Elevated Transit Lines of the New York City Transit Authority," by C.J. Costantino, C.A. Miller and E. Heymsfield, 12/26/89, (PB90-207887/AS).
- NCEER-89-0040 "Centrifugal Modeling of Dynamic Soil-Structure Interaction," by K. Weissman, Supervised by J.H. Prevost, 5/10/89, (PB90-207879/AS).
- NCEER-89-0041 "Linearized Identification of Buildings With Cores for Seismic Vulnerability Assessment," by I-K. Ho and A.E. Aktan, 11/1/89, (PB90-251943/AS).
- NCEER-90-0001 "Geotechnical and Lifeline Aspects of the October 17, 1989 Loma Prieta Earthquake in San Francisco," by T.D. O'Rourke, H.E. Stewart, F.T. Blackburn and T.S. Dickerman, 1/90, (PB90-208596/AS).
- NCEER-90-0002 "Nonnormal Secondary Response Due to Yielding in a Primary Structure," by D.C.K. Chen and L.D. Lutes, 2/28/90, (PB90-251976/AS).
- NCEER-90-0003 "Earthquake Education Materials for Grades K-12," by K.E.K. Ross, 4/16/90, (PB91-113415/AS).
- NCEER-90-0004 "Catalog of Strong Motion Stations in Eastern North America," by R.W. Busby, 4/3/90, (PB90-251984/AS).
- NCEER-90-0005 "NCEER Strong-Motion Data Base: A User Manual for the GeoBase Release (Version 1.0 for the Sun3)," by P. Friberg and K. Jacob, 3/31/90 (PB90-258062/AS).
- NCEER-90-0006 "Seismic Hazard Along a Crude Oil Pipeline in the Event of an 1811-1812 Type New Madrid Earthquake," by H.H.M. Hwang and C-H.S. Chen, 4/16/90(PB90-258054).
- NCEER-90-0007 "Site-Specific Response Spectra for Memphis Sheahan Pumping Station," by H.H.M. Hwang and C.S. Lee, 5/15/90, (PB91-108811/AS).

- NCEER-90-0008 "Pilot Study on Seismic Vulnerability of Crude Oil Transmission Systems," by T. Arıman, R. Dobry, M. Grigoriu, F. Kozin, M. O'Rourke, T. O'Rourke and M. Shinozuka, 5/25/90, (PB91-108837/AS).
- NCEER-90-0009 "A Program to Generate Site Dependent Time Histories: EQGEN," by G.W. Ellis, M. Srinivasan and A.S. Cakmak, 1/30/90, (PB91-108829/AS).
- NCEER-90-0010 "Active Isolation for Seismic Protection of Operating Rooms," by M.E. Talbott, Supervised by M. Shinozuka, 6/8/9, (PB91-110205/AS).
- NCEER-90-0011 "Program LINEARID for Identification of Linear Structural Dynamic Systems," by C.B. Yun and M. Shinozuka, 6/25/90, (PB91-110312/AS).
- NCEER-90-0012 "Two-Dimensional Two-Phase Elasto-Plastic Seismic Response of Earth Dams," by A.N. Yiangos, Supervised by J.H. Prevost, 6/20/90, (PB91-110197/AS).
- NCEER-90-0013 "Secondary Systems in Base-Isolated Structures: Experimental Investigation, Stochastic Response and Stochastic Sensitivity," by G.D. Manolis, G. Juhn, M.C. Constantinou and A.M. Reinhorn, 7/1/90, (PB91-110320/AS).
- NCEER-90-0014 "Seismic Behavior of Lightly-Reinforced Concrete Column and Beam-Column Joint Details," by S.P. Peziki, C.H. Conley, P. Gergely and R.N. White, 8/22/90, (PB91-108795/AS).
- NCEER-90-0015 "Two Hybrid Control Systems for Building Structures Under Strong Earthquakes," by J.N. Yang and A. Danielians, 6/29/90, (PB91-125393/AS).
- NCEER-90-0016 "Instantaneous Optimal Control with Acceleration and Velocity Feedback," by J.N. Yang and Z. Li, 6/29/90, (PB91-125401/AS).
- NCEER-90-0017 "Reconnaissance Report on the Northern Iran Earthquake of June 21, 1990," by M. Mehraın, 10/4/90, (PB91-125377/AS).
- NCEER-90-0018 "Evaluation of Liquefaction Potential in Memphis and Shelby County," by T.S. Chang, P.S. Tang, C.S. Lee and H. Hwang, 8/10/90, (PB91-125427/AS).
- NCEER-90-0019 "Experimental and Analytical Study of a Combined Sliding Disc Bearing and Helical Steel Spring Isolation System," by M.C. Constantinou, A.S. Mokha and A.M. Reinhorn, 10/4/90, (PB91-125385/AS).
- NCEER-90-0020 "Experimental Study and Analytical Prediction of Earthquake Response of a Sliding Isolation System with a Spherical Surface," by A.S. Mokha, M.C. Constantinou and A.M. Reinhorn, 10/11/90, (PB91-125419/AS).
- NCEER-90-0021 "Dynamic Interaction Factors for Floating Pile Groups," by G. Gazetas, K. Fan, A. Kaynia and E. Kausel, 9/10/90, (PB91-170381/AS).
- NCEER-90-0022 "Evaluation of Seismic Damage Indices for Reinforced Concrete Structures," by S. Rodriguez-Gomez and A.S. Cakmak, 9/30/90, PB91-171322/AS).
- NCEER-90-0023 "Study of Site Response at a Selected Memphis Site," by H. Desai, S. Ahmad, E.S. Gazetas and M.R. Oh, 10/11/90, (PB91-196857/AS).
- NCEER-90-0024 "A User's Guide to Strongmo: Version 1.0 of NCEER's Strong-Motion Data Access Tool for PCs and Terminals," by P.A. Friberg and C.A.T. Susch, 11/15/90, (PB91-171272/AS).
- NCEER-90-0025 "A Three-Dimensional Analytical Study of Spatial Variability of Seismic Ground Motions," by L.-L. Hong and A.H.-S. Ang, 10/30/90, (PB91-170399/AS).

- NCEER-90-0026 "MUMOID User's Guide - A Program for the Identification of Modal Parameters," by S. Rodriguez-Gomez and E. DiPasquale, 9/30/90, (PB91-171298/AS).
- NCEER-90-0027 "SARCF-II User's Guide - Seismic Analysis of Reinforced Concrete Frames," by S. Rodriguez-Gomez, Y.S. Chung and C. Meyer, 9/30/90, (PB91-171280/AS).
- NCEER-90-0028 "Viscous Dampers: Testing, Modeling and Application in Vibration and Seismic Isolation," by N. Makris and M.C. Constantinou, 12/20/90 (PB91-190561/AS).
- NCEER-90-0029 "Soil Effects on Earthquake Ground Motions in the Memphis Area," by H. Hwang, C.S. Lee, K.W. Ng and T.S. Chang, 8/2/90, (PB91-190751/AS)
- NCEER-91-0001 "Proceedings from the Third Japan-U.S. Workshop on Earthquake Resistant Design of Lifeline Facilities and Countermeasures for Soil Liquefaction, December 17-19, 1990," edited by T.D. O'Rourke and M. Hamada, 2/1/91. (PB91-179259/AS).
- NCEER-91-0002 "Physical Space Solutions of Non-Proportionally Damped Systems," by M. Tong, Z. Liang and G.C. Lee, 1/15/91, (PB91-179242/AS).
- NCEER-91-0003 "Seismic Response of Single Piles and Pile Groups," by K. Fan and G. Gazetas, 1/10/91, (PB92-174994/AS).
- NCEER-91-0004 "Damping of Structures: Part 1 - Theory of Complex Damping," by Z. Liang and G. Lee, 10/10/91, (PB92-197235/AS).
- NCEER-91-0005 "3D-BASIS - Nonlinear Dynamic Analysis of Three Dimensional Base Isolated Structures: Part II," by S. Nagarajaiah, A.M. Reinhorn and M.C. Constantinou, 2/28/91, (PB91-190553/AS).
- NCEER-91-0006 "A Multidimensional Hysteretic Model for Plasticity Deforming Metals in Energy Absorbing Devices," by E.J. Graesser and F.A. Cozzarelli, 4/9/91, (PB92-108364/AS).
- NCEER-91-0007 "A Framework for Customizable Knowledge-Based Expert Systems with an Application to a KBES for Evaluating the Seismic Resistance of Existing Buildings," by E.G. Ibarra-Anaya and S.J. Fenves, 4/9/91, (PB91-210930/AS).
- NCEER-91-0008 "Nonlinear Analysis of Steel Frames with Semi-Rigid Connections Using the Capacity Spectrum Method," by G.G. Deierlein, S-H. Hsieh, Y-J. Shen and J.F. Abel, 7/2/91, (PB92-113828/AS).
- NCEER-91-0009 "Earthquake Education Materials for Grades K-12," by K.E.K. Ross, 4/30/91, (PB91-212142/AS).
- NCEER-91-0010 "Phase Wave Velocities and Displacement Phase Differences in a Harmonically Oscillating Pile," by N. Makris and G. Gazetas, 7/8/91, (PB92-108356/AS).
- NCEER-91-0011 "Dynamic Characteristics of a Full-Size Five-Story Steel Structure and a 2/5 Scale Model," by K.C. Chang, G.C. Yao, G.C. Lee, D.S. Hao and Y.C. Yeh," 7/2/91.
- NCEER-91-0012 "Seismic Response of a 2/5 Scale Steel Structure with Added Viscoelastic Dampers," by K.C. Chang, T.T. Soong, S-T. Oh and M.L. Lai, 5/17/91 (PB92-110816/AS).
- NCEER-91-0013 "Earthquake Response of Retaining Walls: Full-Scale Testing and Computational Modeling." by S. Alampalli and A-W.M. Elgarnal, 6/20/91, to be published.
- NCEER-91-0014 "3D-BASIS-M: Nonlinear Dynamic Analysis of Multiple Building Base Isolated Structures," by P.C. Tsopelas, S. Nagarajaiah, M.C. Constantinou and A.M. Reinhorn, 5/28/91, (PB92-113885/AS).

- NCEER-91-0015 "Evaluation of SEAOC Design Requirements for Sliding Isolated Structures," by D. Theodossiou and M.C. Constantinou, 6/10/91, (PB92-114602/AS).
- NCEER-91-0016 "Closed-Loop Modal Testing of a 27-Story Reinforced Concrete Flat Plate-Core Building," by H.R. Somaprasad, T. Toksoy, H. Yoshiyuki and A.E. Aktan, 7/15/91, (PB92-129980/AS).
- NCEER-91-0017 "Shake Table Test of a 1/6 Scale Two-Story Lightly Reinforced Concrete Building," by A.G. El-Attar, R.N. White and P. Gergely, 2/28/91, (PB92-222447/AS).
- NCEER-91-0018 "Shake Table Test of a 1/8 Scale Three-Story Lightly Reinforced Concrete Building," by A.G. El-Attar, R.N. White and P. Gergely, 2/28/91.
- NCEER-91-0019 "Transfer Functions for Rigid Rectangular Foundations," by A.S. Veletsos, A.M. Prasad and W.H. Wu, 7/31/91.
- NCEER-91-0020 "Hybrid Control of Seismic-Excited Nonlinear and Inelastic Structural Systems," by J.N. Yang, Z. Li and A. Danielians, 8/1/91, (PB92-143171/AS).
- NCEER-91-0021 "The NCEER-91 Earthquake Catalog: Improved Intensity-Based Magnitudes and Recurrence Relations for U.S. Earthquakes East of New Madrid," by L. Seeber and J.G. Armbruster, 8/28/91, (PB92-176742/AS).
- NCEER-91-0022 "Proceedings from the Implementation of Earthquake Planning and Education in Schools: The Need for Change - The Roles of the Changemakers," by K.E.K. Ross and F. Winslow, 7/23/91, (PB92-129998/AS).
- NCEER-91-0023 "A Study of Reliability-Based Criteria for Seismic Design of Reinforced Concrete Frame Buildings," by H.H.M. Hwang and H.M. Hsu, 8/10/91, (PB92-140235/AS).
- NCEER-91-0024 "Experimental Verification of a Number of Structural System Identification Algorithms," by R.G. Ghanem, H. Gavin and M. Shinozuka, 9/18/91, (PB92-176577/AS).
- NCEER-91-0025 "Probabilistic Evaluation of Liquefaction Potential," by H.H.M. Hwang and C.S. Lee, 11/25/91, (PB92-143429/AS).
- NCEER-91-0026 "Instantaneous Optimal Control for Linear, Nonlinear and Hysteretic Structures - Stable Controllers," by J.N. Yang and Z. Li, 11/15/91, (PB92-163807/AS).
- NCEER-91-0027 "Experimental and Theoretical Study of a Sliding Isolation System for Bridges," by M.C. Constantinou, A. Kartoum, A.M. Reinhorn and P. Bradford, 11/15/91, (PB92-176973/AS).
- NCEER-92-0001 "Case Studies of Liquefaction and Lifeline Performance During Past Earthquakes, Volume 1: Japanese Case Studies," Edited by M. Hamada and T. O'Rourke, 2/17/92, (PB92-197243/AS).
- NCEER-92-0002 "Case Studies of Liquefaction and Lifeline Performance During Past Earthquakes, Volume 2: United States Case Studies," Edited by T. O'Rourke and M. Hamada, 2/17/92, (PB92-197250/AS).
- NCEER-92-0003 "Issues in Earthquake Education," Edited by K. Ross, 2/3/92, (PB92-222389/AS).
- NCEER-92-0004 "Proceedings from the First U.S. - Japan Workshop on Earthquake Protective Systems for Bridges," 2/4/92, to be published.
- NCEER-92-0005 "Seismic Ground Motion from a Haskell-Type Source in a Multiple-Layered Half-Space," A.P. Theoharis, G. Deodatis and M. Shinozuka, 1/2/92, to be published.
- NCEER-92-0006 "Proceedings from the Site Effects Workshop," Edited by R. Whitman, 2/29/92, (PB92-197201/AS).

- NCEER-92-0007 "Engineering Evaluation of Permanent Ground Deformations Due to Seismically-Induced Liquefaction," by M.H. Baziar, R. Dobry and A.W.M. Elgamal, 3/24/92, (PB92-222421/AS).
- NCEER-92-0008 "A Procedure for the Seismic Evaluation of Buildings in the Central and Eastern United States," by C.D. Poland and J.O. Malley, 4/2/92, (PB92-222439/AS).
- NCEER-92-0009 "Experimental and Analytical Study of a Hybrid Isolation System Using Friction Controllable Sliding Bearings," by M.Q. Feng, S. Fujii and M. Shinozuka, 5/15/92, (PB93-150282/AS).
- NCEER-92-0010 "Seismic Resistance of Slab-Column Connections in Existing Non-Ductile Flat-Plate Buildings," by A.J. Durrani and Y. Du, 5/18/92.
- NCEER-92-0011 "The Hysteretic and Dynamic Behavior of Brick Masonry Walls Upgraded by Ferrocement Coatings Under Cyclic Loading and Strong Simulated Ground Motion," by H. Lee and S.P. Prawl, 5/11/92, to be published.
- NCEER-92-0012 "Study of Wire Rope Systems for Seismic Protection of Equipment in Buildings," by G.F. Demetriades, M.C. Constantinou and A.M. Reinhorn, 5/20/92.
- NCEER-92-0013 "Shape Memory Structural Dampers: Material Properties, Design and Seismic Testing," by P.R. Witting and F.A. Cozzarelli, 5/26/92.
- NCEER-92-0014 "Longitudinal Permanent Ground Deformation Effects on Buried Continuous Pipelines," by M.J. O'Rourke, and C. Nordberg, 6/15/92.
- NCEER-92-0015 "A Simulation Method for Stationary Gaussian Random Functions Based on the Sampling Theorem," by M. Grigoriu and S. Balopoulou, 6/11/92, (PB93-127496/AS).
- NCEER-92-0016 "Gravity-Load-Designed Reinforced Concrete Buildings: Seismic Evaluation of Existing Construction and Detailing Strategies for Improved Seismic Resistance," by G.W. Hoffmann, S.K. Kunnath, J.B. Mander and A.M. Reinhorn, 7/15/92, to be published.
- NCEER-92-0017 "Observations on Water System and Pipeline Performance in the Limón Area of Costa Rica Due to the April 22, 1991 Earthquake," by M. O'Rourke and D. Ballantyne, 6/30/92, (PB93-126811/AS).
- NCEER-92-0018 "Fourth Edition of Earthquake Education Materials for Grades K-12," Edited by K.E.K. Ross, 8/10/92.
- NCEER-92-0019 "Proceedings from the Fourth Japan-U.S. Workshop on Earthquake Resistant Design of Lifeline Facilities and Countermeasures for Soil Liquefaction," Edited by M. Hamada and T.D. O'Rourke, 8/12/92, (PB93-163939/AS).
- NCEER-92-0020 "Active Bracing System: A Full Scale Implementation of Active Control," by A.M. Reinhorn, T.T. Soong, R.C. Lin, M.A. Rizky, Y.P. Wang, S. Aizawa and M. Higashino, 8/14/92, (PB93-127512/AS).
- NCEER-92-0021 "Empirical Analysis of Horizontal Ground Displacement Generated by Liquefaction-Induced Lateral Spreads," by S.F. Bartlett and T.L. Youd, 8/17/92.
- NCEER-92-0022 "IDARC Version 3.0: Inelastic Damage Analysis of Reinforced Concrete Structures," by S.K. Kunnath, A.M. Reinhorn and R.F. Lobo, 8/31/92.
- NCEER-92-0023 "A Semi-Empirical Analysis of Strong-Motion Peaks in Terms of Seismic Source, Propagation Path and Local Site Conditions," by M. Kanayama, M.J. O'Rourke and R. Flores-Berrones, 9/9/92, (PB93-150266/AS).
- NCEER-92-0024 "Seismic Behavior of Reinforced Concrete Frame Structures with Nonductile Details, Part I: Summary of Experimental Findings of Full Scale Beam-Column Joint Tests," by A. Beres, R.N. White and P. Gergely, 9/30/92.
- NCEER-92-0025 "Experimental Results of Repaired and Retrofitted Beam-Column Joint Tests in Lightly Reinforced Concrete Frame Buildings," by A. Beres, S. El-Borgi, R.N. White and P. Gergely, 10/29/92.